Progressive Disc Herniation: An investigation of the mechanism using histochemical and microscopic techniques

By

Claudio Tampier

A thesis
presented to the University of Waterloo
in fulfillment of the
thesis requirement for the degree of

Master of Science
in
Kinesiology

Waterloo, Ontario, Canada, 2006

I hereby declare that I am the sole author of this thesis.

I authorize the University of Waterloo to lend this thesis to other institutions or individuals for the purpose of scholarly research.

Claudio Tampier

I further authorize the University of Waterloo to reproduce this thesis by photocopying or by other means, in total or in part, at the request of other institutions or individuals for the purpose of scholarly research.

Claudio Tampier

Abstract

Background: The process that involves the migration of the nucleus pulposus from the innermost annular layers and culminates with the final extrusion of the nucleus has been limited to a few studies. This investigation was directed towards a better understanding of the herniation process. The architecture of the annulus fibrosus and the mechanism of progressive disc herniation were analyzed, using a controlled porcine model. Microscopic and histochemical techniques were employed.

Methodology: Two studies were performed. In the first stage, the macroscopic and microscopic structures of twelve cervical intervertebral discs were compared with young human disc data from studies reported in the literature. Important structural features were studied such as annulus fibrosus thickness, number of lamellae, lamellae thickness, orientation of the lamellae fibers and blood supply. In the second study, sixteen fresh-frozen functional spine units were submitted to repetitive flexion–extension motions combined with a low compressive load in a servo-hydraulic dynamic testing system. Discograms, dissections and histochemical techniques were applied to characterize the cumulative damage. The experiment produced eight complete herniations, four partial herniations and four specimens without any microscopic detectable annular damage.

Results and Discussion: The structure of the cervical porcine disc resembles the lumbar human disc. Some differences are evident. The size of the annulus is smaller, the thickness of the lamellae is narrower and the number of layers is fewer in the pig. It

is hypothesized that the flexion-extension motion combined with a low-level load produced an increased hydraulic pressure in the inner wall of the posterior annulus. This pressure and repetitive motion first produced a small cleft, spreading the collagen bundles inside the first layer. The nuclear material was "pumped" through the small cleft to the first layer filling the layer creating a fluid-filled pocket between the collagen fibers. Once the "pocket" acquired enough pressure a new cleft was produced in the weakest part of the layer allowing the nuclear material to create a new "pocket" in the second layer. This was the first stage of damage and disc herniation production. This mechanism was repeated until the nucleus traveled along the annulus reaching the posterior longitudinal ligament. At this point a complete extrusion herniation was produced.

Conclusion: The porcine model appears to be suitable as a model to understand the mechanism of disc herniation when the spine is subjected to flexion-extension motions combined with a low-level load. The first cumulative injury appears to be a cleft between the lamellae bundles produced by the nuclear hydraulic pressure. A cumulative load/cumulative injury model approach was used to create the damage that was quantified in the study.

Acknowledgements

First and foremost, I would like to thank Dr. Stuart McGill, my supervisor, for sharing his insights and expertise over the two years we have worked together. I also would like to thank my committee members, Dr. Jack Callaghan and Dr. Clark Dickerson who were generous in sharing their time and expertise.

I would like to express my sincere appreciation to Janice Flynn and Janessa Drake who were a great support during this Master of Science program.

I would like to thank my employers, Asociación Chilena de Seguridad and Universidad Austral de Chile for there important support and trust.

Mentioned last in the order, but primary in importance are my wife Paula and children Carla, Marcelo, Felipe and Sofía whose unquestioned support and understanding were the underlying reassurance upon which I could always depend.

Contents

List of Tables

List of Figures

1-INTRODUCTION

Lumbar disc herniation is the last stage of cumulative trauma in an adult intervertebral disc that possesses hydraulic behavior. The process involves the migration of the nucleus pulposus. The migration appears to begin at the innermost annular layers and culminates with the final extrusion of the nucleus. The extruded material may enter the vertebral canal which can compress or irritate the lumbar spinal roots producing radiating sciatica. Current knowledge of the mechanism behind the migration of the nucleus pulposus is limited to only a few studies. Most studies utilize cadavers providing harvested specimens of different ages and levels of disc degeneration. Some specimens possess partial or protruded disc herniations but the time of the occurrence of these in the donor's life is unknown. This investigation is directed towards better understanding the herniation process.

Fatigue failure occurs by accumulation of micro-damage caused by repetitive application of forces and moments which are too small to cause detectable damage if applied only once. Adams and Hutton (1985) produced gradual disc prolapse by applying compression loading and repetitive bending motion in cadaveric lumbar functional spine units (FSU). The authors monitored the gradual prolapse by direct observation and discogram, and found the injury started with the lamellae of the annulus being distorted to form radial fissures. The nuclear pulp was then extruded from the disc and sometimes into the spinal canal (Figure 1.1). Discs most commonly affected were from lower lumbar spinal level of young cadavers. Gordon et al. (1991) applying the same approach (highly repetitive and relatively low level combined loading) but using a more physiologically representative loading protocol, produced

annular protrusions and nuclear extrusion through annular tears. This work supports the hypothesis that intervertebral disc prolapse proceeds progressively from the inside outwards.

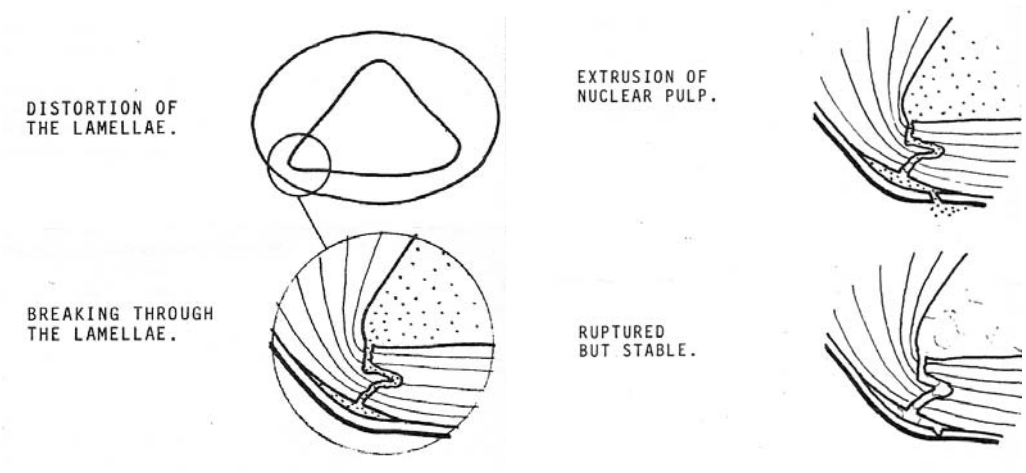

Figure 1.1. Stages of gradual disc prolapse. (Adams, M.A., Hutton, W.C., 1985. Gradual disc prolapse. *Spine* 10, 524-531)

The use of human spine specimens for testing presents some limitations, such as the non-homogeneity in obtained samples. This has motivated the development of a suitable animal model as a source of spine specimens where control can be exercised over genetic homogeneity, physical activity, general health, diet, and weight.

Mammalian discs appear to be quite similar in basic architecture in all species. Although the discs develop in a similar manner in the embryo, changes occur and result in detailed differences between species (Butler, 1988). Several animal models have been developed to replicate injuries in the vertebral spine including canine (Hasegawa et al. 2000), rodent (Iatridis et al. 1999), lagomorph (Kroeber et al. 2002), ovine (Osti et al. 1990, Reid et al. 2002), bovine (Allan et al. 1990), and porcine (Oxland et al. 1991, Lundin et al. 2000, Holm et al. 2004, Panjabi et al. 1989). From our own laboratory,

Yingling et al. (1999) compared the anatomical, geometric and functional characteristics of the porcine cervical spine with the human spine. The porcine cervical vertebral motion segment model shared several parameters with the human lumbar vertebral motion segment, but there are no studies comparing the disc structure between these two models, particularly from the perspective of the mechanism of herniation. Porcine tissues share enough characteristics with human tissue to allow them to be used to replace damaged tissues in humans. While being an immunological discordant species to human, the anatomical, physiological and biochemical characteristics between pigs and humans show some compatibility (Lambrigts et al. 1998). Pigs have the advantage over non human primates as potential donors for human xenotransplant (a transplant between species), as they can be easily genetically manipulated (unlike primates) to express extrinsic genes, which could address some of the barriers to xenotransplant (Samstein et al. 2001). Experiments in pigs suggest there is potential in the future for the use of different organs for xenotransplantation, such as liver, kidney, heart and by inference, the intervertebral disc.

This thesis documents the efforts to better understand the architecture of the annulus fibrosus and the mechanism of progressive disc herniation using a controlled porcine model. Microscopic and histochemical techniques were employed.

1.1-Pupose

The purpose of this study is twofold.

1. To quantify and describe the architecture of the cervical porcine intervertebral disc. To evaluate the resemblance and appropriateness of this model by comparing the

macroscopic and microscopic structure of the porcine spines with the data of young human lumbar discs from studies reported in the literature.

2. To understand the mechanism of how damage to the annulus is produced under combined motion and loads (flexion/extension motions and compressive forces) from an anatomical-pathological perspective. The damage to the annulus fibrosus is characterized with the use of precision dissection and microscopic techniques together with histochemical staining techniques. The cascade of cumulative trauma is documented from the first microscopic damage to eventual nucleus pulposus extrusion.

1.2 Hypothesis

1- The structure of the intervertebral disc of the cervical spine of the pig will resemble the structure of the disc of human lumbar spine. Some differences in the size and number of lamellae will be evident. The size of the annulus will be smaller, the thickness of the lamellae will be narrower and the number of layers will be fewer.

2- Highly repetitive flexion-extension motions with relatively low magnitudes of compressive forces will first produce a radial cleft in the annulus fibrosus, then disc delamination where the nucleus pulposus is displaced and accumulates finally nuclear extrusion. The degree of damage will depend on the variables: number of cycles, cumulative load applied, and time exposed, which will support a cumulative load/ cumulative injury model.

3- The delamination of annular layers will appear to be due to hydraulic stresses from nuclear liquids rather than from applied motions and loads.

2- REVIEW OF RELATED LITERATURE

2.1- Epidemiology

Low back pain is experienced by 80% of the population at some time during their working lives, and by 30-40% of any workforce (Hadler et al. 1986). Epidemiological studies have found that repetitive compression loading (Jager et al. 2000, Norman et al. 1998) and axial rotation and velocity (Marras et al. 1993, Punnett et al. 1991) were considered to be the most important contributing factors for development of spine and disc injuries.

Biering-Sørensen (1983) studied all of the inhabitants from 30 to 60 years of age in a Copenhagen suburb in Denmark, and found the lifetime prevalence rate for low back pain ranged from 68% to 70% for men and from 62% to 81% for women. The incidence of first attacks of low back pain over the follow-up years was highest in the 30-year-olds at 11%, and decreased in the older age groups. Heavy lifting, twisting and trauma were the most commonly stated causes of low back pain, and 52- 60% of these were reported to be work related. Murphy et al. (1998) estimated the cost of low back claims in the United States in 1995 at $8.8 billion. Lumbar disc herniation is the diagnosis most frequently given to patients with lumbar radiculopathy and is the most common reason for lumbar spine surgery (Postacchini et al. 2001).

However, Porter (1987) in a prevalence study that compared the risk of disc protrusion between heavy workers (coal miners), and non heavy workers found manual heavy workers had less risk of disc protrusion and less surgical excisions. The author suggested the need to identify and encourage activities in early life which may develop annular and ligamentous strength.

These epidemiologic studies suggested the relationship of low back tissue loading to injury risk appears to form a U-shaped function with an optimum somewhere between “too much and too little”. Evidence postulates that heavy work is good for the back but only with appropriate dosage, too much and too little could be the source of disc injury.

2.2- Review of the Anatomy

2.2.1- The Lumbar Vertebrae

The lumbar vertebral column consists of five separate vertebrae, which are named according to their location in the intact column. The typical lumbar vertebra is composed by the vertebral body, a short, cylindrical block of bone that is flattened at the back and possesses a slight “waist” (Figure 2.1). Adjacent bodies are firmly united to one another by an intervertebral disc, roughly one fifth to one third as thick as the neighboring bodies. Projecting from the back are two stout pillars of bone, each called a pedicle, and in the posterior part these form a bridge of bone called a lamina. The two laminae meet and fuse with one another at the midline from which the spinous process protrudes posteriorly. The lateral and inferior border of each lamina is developed into a specialized mass of bone, the inferior articular process. Extending upwards from the junction of the lamina and pedicle on each side is a superior articular process. Each vertebra presents four articular processes. On the medial surface of each superior process and on the lateral surface of each inferior process is a smooth area of bone which in the intact spine is covered by articular cartilage. This area is known as the articular facet of each articular process. The transverse process is a flat rectangular bar

that attaches to the junction of the pedicle and lamina on each lateral side. Near its attachment to the pedicle, each transverse process bears on its posterior surface a small, irregular prominence called the accessory process. Viewing a vertebra from above, it can be seen that the neural arch and the back of the vertebral surround a space called vertebral canal that transmits and protects the spinal cord.

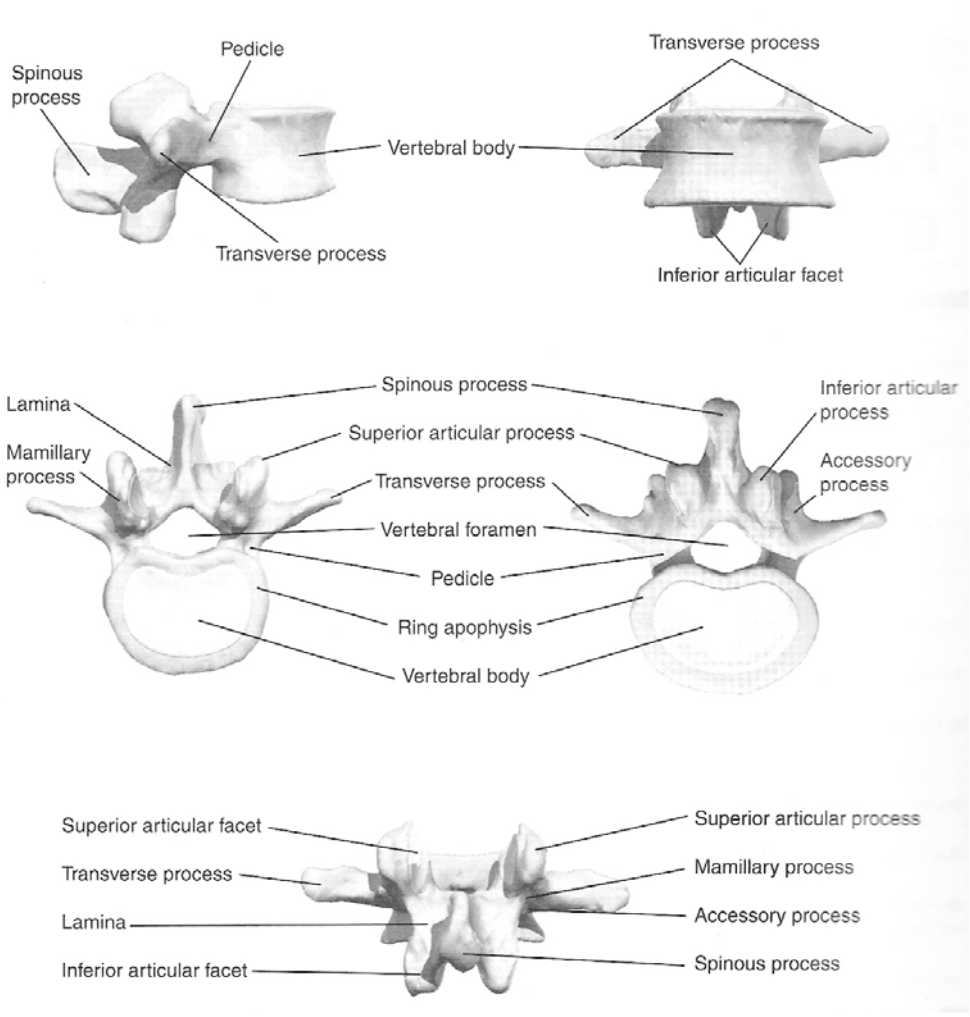

Figure 2.1. Anatomy of a lumbar vertebra (McGill, S.M., 2002. Low back disorders. Evidence-based prevention and rehabilitation. Human Kinetics. Windsor. Pg. 46)

2.2.2- The Intervertebral Disc

The biomechanical requirements of an intervertebral disc are threefold. First, it must bear load, and transfer the load to the next vertebral body without collapsing. Second, it must be deformable to accommodate the rocking and twisting movements of the vertebrae. Thirdly, it must be sufficiently strong so it will not be injured during movement (Adams et al. 2002).

The intervertebral disc (IVD) consists of three different structures: the nucleus pulposus (NP) surrounded by a peripheral annulus fibrosus (AF), and the end plates (EP) which covers the top and the bottom aspects of each disc (Figure 2.2).

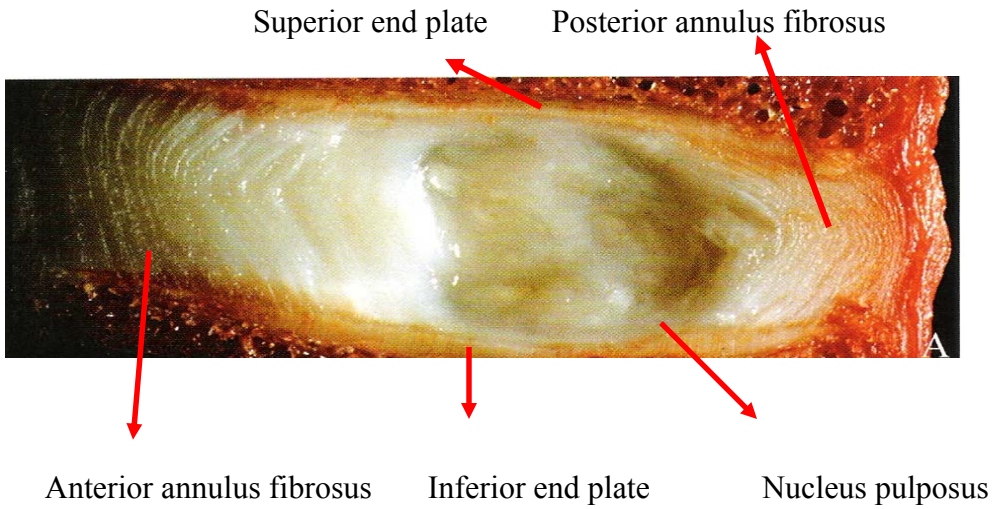

Figure 2.2. Intervertebral disc, sagittal section. (Adams, M.A., et al., 2002. The biomechanics of back pain. Churchill Livingstone, Toronto).

The nucleus pulposus is a semi-fluid mass of mucoid material formed by a few cartilage cells and some irregularly arranged collagen fibers that are dispersed in a medium of semi fluid ground substance. The glycosaminoglycans (GAG) are an

important constituent of the nucleus. They are long chain of polysaccharides, each chain consisting of a repeated sequence of a sugar molecule, and a sugar molecule with an amine attached (Figure 2.3). The GAGs found in human intervertebral discs are chrondroitin-6-sulphate, chrondoitin-4-sulphate, keratan sulphate and hyaluronic acid

The proteoglycans are very large molecules consisting of many glycosaminoglycans linked to proteins. Proteoglycan aggregates are formed when several proteoglycan units are linked to a chain of hyaluronic acid. Physicochemically, these molecules have the property of attracting and retaining water.

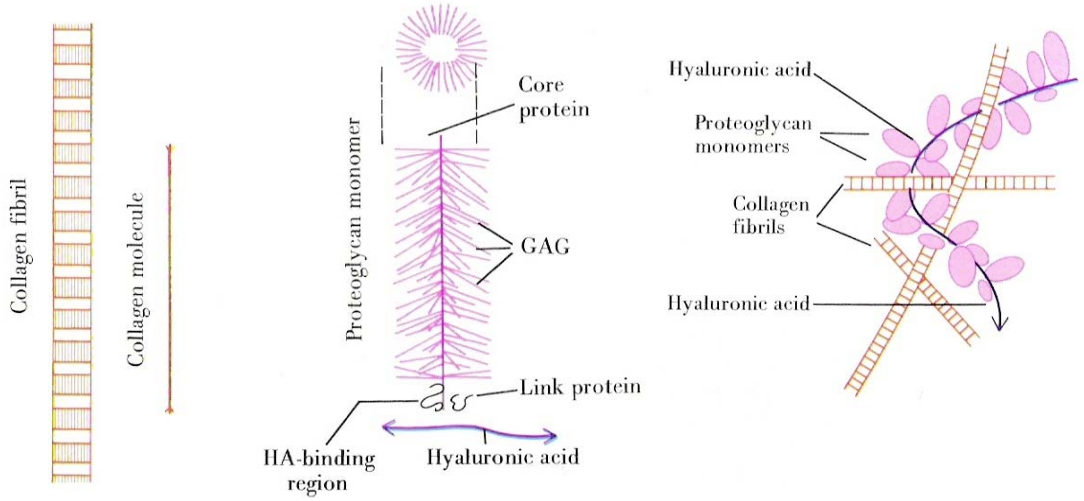

Figure 2.3. Schematic diagram showing a model for the organization of ground substance. On the left a collagen fibril and a collagen molecule are depicted for reference. The next item shows a proteoglycan monomer, hialuronic acid (HA), and a link protein. On the right, an HA molecule forming a linear aggregate with many proteoglycan monomers is interwoven with a network of collagen fibrils. (Hascall et al: Biological Mineralization and Demineralization. New York, Springer, 1982, p. 181.)

The collagens are a family of closely related proteins which can aggregate to produce either filaments, fibrils or mesh-works, which then interact with other proteins to provide support in the extracellular matrix.

The collagen structure consists of strands of protein molecules in which tropocollagen is the fundamental unit. It consists of three polipeptides chains wound around one another in an helical fashion. When only few tropocollagen chains are arranged side by side, the structure formed is known as a small collagen fibril. When the structure is made thicker, by the addition of further layers of tropocollagen chains, it is referred to as a large fibril. Several large fibrils aggregated together form a collagen fiber. The tropocollagen chains within a collagen fiber are held together, side by side, by covalent hydrogen bonds involving a molecule of hydroxylysine.

There are different types of collagen in the intervertebral disc, eleven types have been described, with the most common being Type I and Type II. While Type I and II are both present in the annulus fibrosus, Type I is the predominant form. Type II is the predominant form in the nucleus pulposus. This is important because these collagen Types have unique chemical structures, enabling differential histochemical staining of the annulus fibrosus and nucleus pulposus (Ross, 1989) (Figure 2.4).

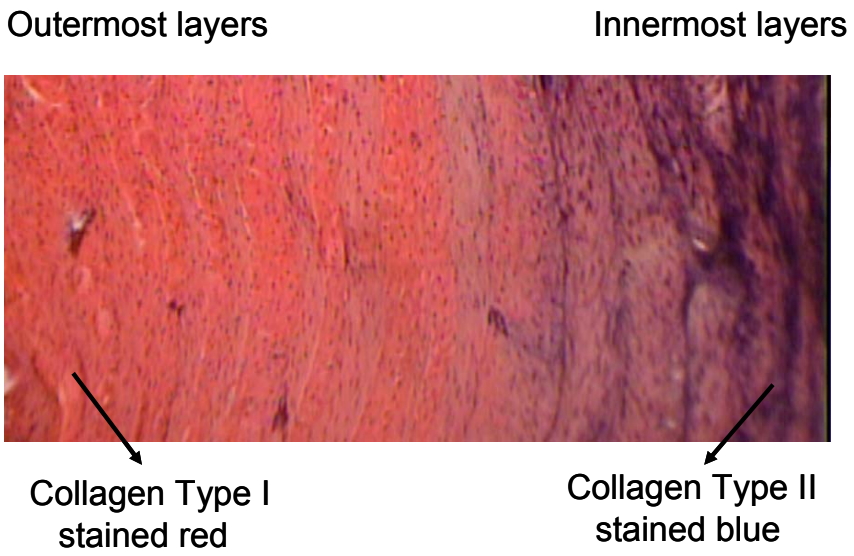

Figure 2.4. Posterior annulus fibrosus stained with hematoxyline and eosin show Type I and Type II collagen distribution.

2.2.3- Microstructure of the Nucleus Pulposus

The nucleus pulposus is approximately 70-90% water, with the exact fraction varying with age. The proteoglycans constitute about 65% of the dry weight of the nucleus. Collagen constitutes 15-20% of the dry weight of the nucleus, and the remainder of the nucleus consists of some elastics fibers and small quantities of non collagenous proteins. The cartilage cells are embedded in the proteoglycan medium and are responsible for the synthesis of proteoglycans and collagen of the nucleus pulposus. They are located predominantly in the region of the vertebral end plate.

2.2.4- Microstructure of the Annulus Fibrosus

Water is also the principal structural component of the annulus fibrosus, amounting to 60-70% of its weight. Collagen represents 50-60% of the dry weight of the annulus. The tight spaces between collagen fibers and between separate lamellae are filled with proteoglycan gel, which binds the collagen fibers and lamellae together to prevent them buckling or fraying. Typically, the annulus consists of about twelve to twenty coaxial lamellae which form a tube enclosing the nucleus. Each lamella contains parallel collagen fibers which are tilted with respect to the spinal axis direction; the direction of tilt alternates from one lamella to the next (Figure 2.5). This pattern of tilted fibers can be observed by dissection of the disc, since individual fibers can be distinguished with naked eye, as well as by light microscopy. Studies have shown that the annular fibers are tilted by about 60 to 70° with respect to the spinal axis direction but the radial and intralemellar variation of inclination angle have been reported to range from 20^{o} to 70^{o}. (Ghosh et al. 1988, Marchand et al. 1990, Bogduk et al. 1991,

Adams et al. 2002). There is also a circumferential variation in the number of lamellae, with the smallest number in the posterior and the greatest, up to as many as 40, in the lateral region of the disc (Hsu et al. 1999).

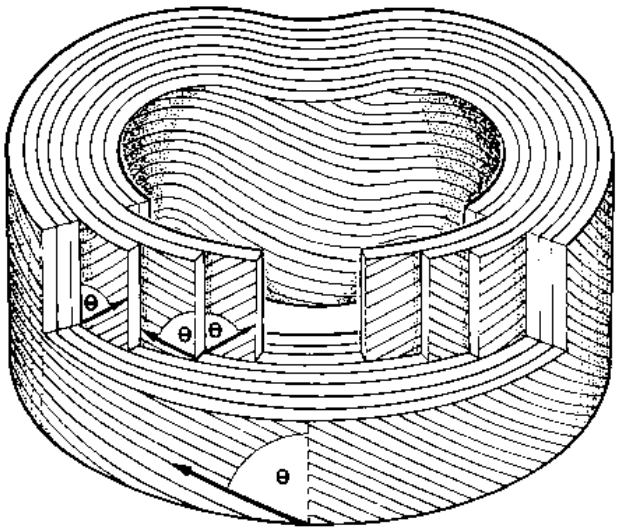

Figure 2.5. The detailed structure of the annulus fibrosus. Collagen fibers are arranged in 10-12 concentric circumferential lamellae. The orientation of fibers alternates in successive lamellae, but their orientation with respect to vertical (θ) are always the same, and measure about 65º. (Bogduk, N., Twomey, L.T. 1991. Clinical Anatomy of the Lumbar Spine. Churchill Livingstone. New York. pg. 13).

The proteoglycan gel between the lamellae acts as the glue in a layer composite, and makes up about 20% of the dry weight of the annulus and it is this gel that binds water of the annulus. Although the annulus and the nucleus are quite different in texture, their boundary is not clearly defined. Inner lamellae of the annulus are attached to the end plates to form a closed vessel containing the nucleus. In contrast, the outer lamellae are attached to the bone of the vertebral bodies. This difference in attachment suggests that there may be some difference in function between the inner and outer regions of the annulus (Hukins, 1988).

From a biochemical perspective, it can be seen that the nucleus pulposus and annulus fibrosus are similar. Both consist of water, collagen and proteoglycan. The differences lie only in the relative concentrations of these components, and in the particular type of collagen that is predominant in each part. The annulus fibrosus also contains a notable quantity of elastic fibers that represent about the 10% of the structures, and are arranged circularly, obliquely and vertically within the lamellae of the annulus (Johnson et al. 1985). They appear to be concentrated towards the attachment sites of the annulus with the vertebral end plate.

The annulus fibrosus is a biologically active structure, however the only vessels that enter the disc are small branches from metaphysical arteries which anastomose over the outer surface of the annulus fibrosus. Consequently, for their nutrition, intervertebral discs are dependent on diffusion from two systems of vessels: those in the outer annulus, and the capillary plexuses beneath the vertebral end plate (Bogduk, 1991).

2.2.5- Vertebral End Plates

The end plate consists of hyaline cartilage with the same chemical structure of the rest of the disc. It is constituted by proteoglycans which resist deformation by compressive forces and collagen fibers which confer mechanical stability. Thus, end plates are reminiscent of the articular cartilage of synovial joints. Due to the attachment of the annulus fibrosus to the end-plates, the end plates are strongly bound to the intervertebral disc. However, in complete contrast to articular cartilage, which is firmly attached to the subchondral bone by its collagen fibrils, there are no collagenous

connections directly anchoring the end-plates to the bone of the underlying vertebral bodies. The end plate resembles the rest of the disc by having a higher concentration of water and proteoglycans and lower collagen content towards its central region that covers the nucleus pulposus, with a reciprocal pattern over the annulus fibrosus. The arrangement of extracellular matrix in cartilage confers important properties. The tightly bound proteoglycans form a hydrated matrix with an inherent turgor that resists deformation by compressive forces and enables small molecules to diffuse freely through the extracellular matrix. Over some of the surface area of the vertebral end-plate (about 10%), the subchondral bone of the vertebral body is deficient and pockets of the marrow cavity abut against the surface of the end plate. These pockets facilitate the diffusion of nutrients from blood vessels in the marrow space, and are important for the nutrition of the end-plate and intervertebral disc (Bogduk et al. 1991).

In general, connective tissues consist of fibroblasts, connective tissue macrophages, mast cells and plasma cells and extracellular fibers embedded in a matrix of coextensive ground substance and tissue fluid. In specialized connective tissues, such as tendon, cartilage, bone and intervertebral disc, where their mechanical function is the most important, the connective tissue presents a well developed amount of extracellular fibers and ground substance. The fibroblast is the cell that produces the extracellular fibers in the annulus and the chondroblast is the cell that produces the extracellular material in the nucleus pulposus (Ross, 1989).

2.3- Review of Pathogenesis of Disc Herniation

Mixter and Barr in 1934 published for the first time a case of a prolapsed intervertebral disc. Barr, in 1954, after preparing a review of vertebral instability as a cause of vertebral laminectomy, claimed at this time that clinical experience had shown that disc lesions (i.e., prolapses) drastically out number all other causes of low back and sciatic pain (Crock, 1986).

Disc herniation in a young population is infrequent. Parisini et al. (2001) reviewed 5160 patients that underwent surgery for lumbar disc herniation, 129 cases were subjects between 9 and 18 years of age. The authors reported that one of the most likely factors accounting for the early onset of lumbar disc herniation was an association with vertebral deformities, such as scoliosis, transitional defects (lumbarization and sacralization), and canal narrowing. In these cases the reported incidence ranged from 30% to 70% (De Orio et al. 1982, Ebersold et al. 1987). Nevertheless, the incidence of early onset of lumbar herniation drops to 15% in a healthy population. These alterations can lead to anomalous biomechanical conditions, both from the static and from the dynamic point of view, thus facilitating disc degeneration and secondary herniation.

The biomechanical aspects of the intervertebral disc have been the subject of intensive investigation, but the same cannot be claimed for its structure. In 1931, Beadle reported that the annulus consists of a number of concentric collagen fiber bundles, displaying a criss-cross pattern. Since then, the gross geometry of the disc and fiber inclination angle was studied by Coventry et al. (1945). Marchand and Ahmed (1990) performed a detailed investigation of the structure of the lumbar disc annulus

fibrosus using a layer by layer technique and microscopic examination of various cut surfaces in both young and old specimens. They found the annulus, excluding the transition zone, consisted of 15 to 25 distinct layers, depending on the circumferential location, the spinal level, and the specimen's age. The inclination of the fiber bundles varies from 0° to 90° and the mean thickness of individual layers varies greatly throughout the annulus. A significant increase in the layer thickness occurred with increasing proximity to the center of the disc. On average, the layer thickness of young discs varies from 0.14mm near the periphery to 0.20 mm near the center of the disc.

Lumbar disc herniation occurs primarily in the posterior region of the intervertebral disc (85-90%) (Haughton, 1988). This may be the consequence of an increased pressure during mechanical loading that surpasses the strength of the posterior annulus fibrosus. A localized weakness in the disc structure or an inherited predisposition could be factors to explain the occurrence of disc herniation in the young population. Tsuji et al. (1993) performed a morphologic comparison of the laminated structure of the anterior and posterior annulus fibrosus of a lumbar intervertebral disc in a fetus, one child, and one young adult cadaver. They found the number of lamellar bundles was greater in the anterior annulus than in the posterior annulus, and a complex structure was observed in the posterior in the posterior-middle annulus in all of the specimens. They concluded that the risk of posterior rupture in the young may be influenced by an inherent structural variation such as a weak posterior annulus fibrosus.

There is universal agreement that acute direct compressive loading of the lumbar motion segment does not cause direct damage to the annulus. (McGill, 2002, Brinckmann et al. 1989, Aultman et al. 2004). The disc has a higher compressive

strength than the vertebral bodies, so under excessive compressive loading the end plate will fracture in a stellate pattern.

Several authors have proposed hypotheses for disc herniation. In Kirkaldy-Willis (1988) textbook it is proposed that recurrent rotational strains first produce a number of small circumferential tears in the annulus fibrosus. Later, these become larger and coalesce to form radial tears that pass from the annulus into the nucleus pulposus. The normal disc height is greatly reduced due to a loss of proteoglycans and water from the nucleus. The annulus becomes lax and bulges around the circumference of the disc. Depending on the amount of support from the annulus, the force applied to the disc, and the viscosity of the nucleus, nuclear material can be displaced. The posterior annulus and the cartilaginous endplate are two sites of potential weakness in the intervertebral disc complex.

Hickey and Hukins (1980), using a model based on the observed arrangement of collagenous fibers in the annulus fibrosus, treated these fibers as if they behave like tendons. They made some predictions about disc failure; torsion and bending could cause failure of the annulus fibrosus and hence protrusion of the nucleus pulposus. Failure is likely to occur posteriorly due to the effect of forward bending. Bending is potentially damaging because it concentrates stress on a limited number of collagenous fibres. Torsional stress is transmitted only to those collagen fibers that are angled in the direction of the applied torque and these fibers represent about half the total number of bundles. Drake et al. (2005), using a porcine model, applied repetitive flexion-extension motion combined with low compression and axial torque to produce disc herniation.

When axial torque was applied disc herniations were more prompt to occur (71%) compared to the no axial torque group (29%).

Although there is broad consensus of the importance of annular lesions among the macroscopic and microscopic features of intervertebral disc herniation, the origin and sequence of their development is significantly more controversial. There is a lack of agreement as to the identity of the herniated material. Friberg and Hirsh (1992) suggested that the annulus ruptures started in the inner annulus and were directed either sagitally or laterally outward toward the periphery. This concept was explained by Galante (1967) as a result of the combination of internal pressure and early failure of the inner annulus fibers caused by degenerative changes. Moore (1996) in a clinicopathologic study, examined disc tissue collected from surgery and from cadaveric spines. The authors concluded that at least in adult subjects, nuclear fragments migrate along preexisting radiating tears of the annulus. Nuclear degeneration first becomes evident as a large cleft toward the periphery of the nucleus as it becomes less hydrated and shrinks, followed by nuclear clefting and fragmentation, which are well established by the third decade of life. Isolated fragments of annulus and end plate are much less common than nucleus extruded material and probably also originate as part of degenerative processes.

Yasuma et al. (1986) histologically examined intervertebral discs obtained at autopsy and material obtained from adult spine surgery. The researchers described the bundle in the internal layer of the annulus fibrosus reversed their usual direction and showed myxomatous degeneration, sometimes resulting in posterior and convex bulging in the internal layer of the anterior and posterior parts of the annulus fibrosus,

respectively. These abnormalities were seen in subjects over the age of fifty. These results suggested that a protrusion herniation type of the annulus fibrosus exists in which only the annulus fibrosus is protruded due to reversal of bundles of the annulus fibrosus, without the involment of the nucleus pulposus. This type of herniation would be a separate entity from the protrusion type of herniation that occurs when the nucleus pulposus is protruded through a fissure in the annulus fibrosus (Figure 2.6).

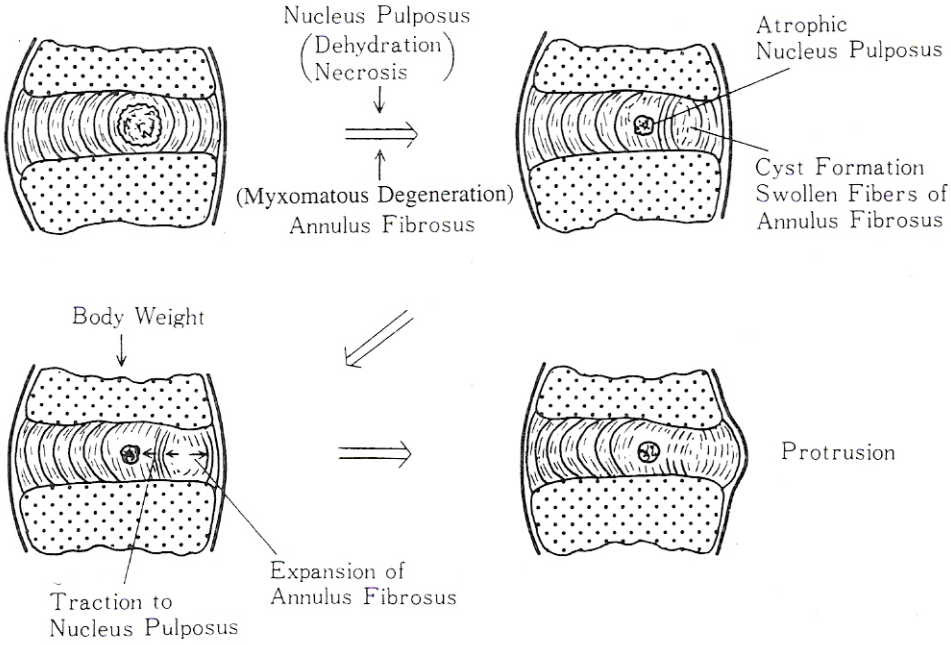

Figure 2.6. Pathomechanism of herniation with protrusion of the annulus fibrosus. (Yasuma et al., 1986 *The Journal of Bone and Joint Surgery* 68-A 1066-1072).

Finally, Lipson (1987) in a more bold hypothesis based on experimental intervertebral degeneration asserted that herniated disc material is actually newly synthesized proliferative metaplastic fibrocartilage and not of pre-existing disc tissue, particularly that of the nucleus pulposus. Surgical tissues from intervertebral disc herniations were examined. The hidroxypyridinium cross-link assay was used to

determine the maturity of the collagen. The result showed that the herniated disc material was a younger tissue than the in situ annulus fibrosus.

Clearly, there have been various observations but no clear mechanism for the process of disc herniation has been described. This has motivated the research proposed for this thesis.

2.4- Review of Staining with Harry's Haematoxyline Solution and Eosin

Fixed protein has approximately the same refractive index as glass, so when examining a stained section under the microscope, it is not the tissue per se that is seen but dye particles attached to the protein molecules that are visible. The majority of tissue reactions involve some form of electrostatic mechanism, so that a cationic (positive charge) dye will bond to anionic (negative charge) tissue. Conversely, anionic dyes will bond cationic tissue.

Haematoxyline and eosin (H & E) staining usually denotes staining of nuclei by oxidized haematoxyline (haematein) through mordant (chelate) bonds of metals such as aluminium, followed by counterstaining by the xanthene dye eosin, which colors in varying shades the different tissue fibers and cytoplasms. Being anionic, the haematein will have no particular affinity for the nucleic acid of cell nuclei. Therefore it is also necessary to combine a metallic salt or mordant with the haematoxyline, which will confer a net positive charge to the dye compound by virtue of the metal cation present. Thus the cationic dye-metal complex will bind to the anionic nuclear chromatin. The haematoxyline solutions are complex and will contain one or more of the following substances, an alum, an acid, an oxidizing agent and glycerol (Bancroft, 1984).

Eosin is an anionic dye and combines electro-statically with tissue such as collagen and muscle. By raising the pH of the solution, eosin will stain more intensely. Haematoxyline stains the nuclei and ground substance blue but only when it is present in large amounts such as in cartilage matrix or nucleus pulposus (Ross, 1989). Eosin stains in differents colours: bright red the nuclei cytoplamic RNA, and the coarse elastic fibers and fibrin; in pink the collagen, the reticulin, the mielinated nerve fibres, and the amyloid; and in orange the red bloods cells.

Haematoxyline and eosin staining technique have been used extensively to study connectives tissues, and some researchers have used the H & E technique to characterize the intervertebral disc (Gunzburg et al. 1992, Hasegawa et al. 2000, Johnson et al. 1985, Yasuma et al. 1986).

3- Materials and Methods

3.1 Summary Study 1.

A precise description, with the use of microscopic techniques together with histochemical staining techniques, was performed. The macroscopic and microscopic structure of the cervical porcine intervertebral disc was compared with young human disc data from studies reported in the literature to evaluate the resemblance and thus appropriateness of this animal model (Cassidy et al. 1989, Marchand et al. 1990, Bogduk et al. 1991, Tsuji et al. 1993, Adams et al. 2002).

In brief, three fresh frozen porcine cervical spines were prepared from C3 to C7 without applying any prior load. The neurological arches were removed with a saw and each vertebral body was cut across the middle of the vertebra in the transverse plane (Figure 3.1). The modified functional spine units C3-C4, C4-5, C5-6, and C6-7 were further sectioned into right/left blocks. The right side was used for histological analysis and the left side was used for macroscopic and microscopic dissection (Figure 3.2). Haematoxyline and eosin staining techniques were performed. Digital pictures were taken to characterize and measure features of the intervertebral disc.

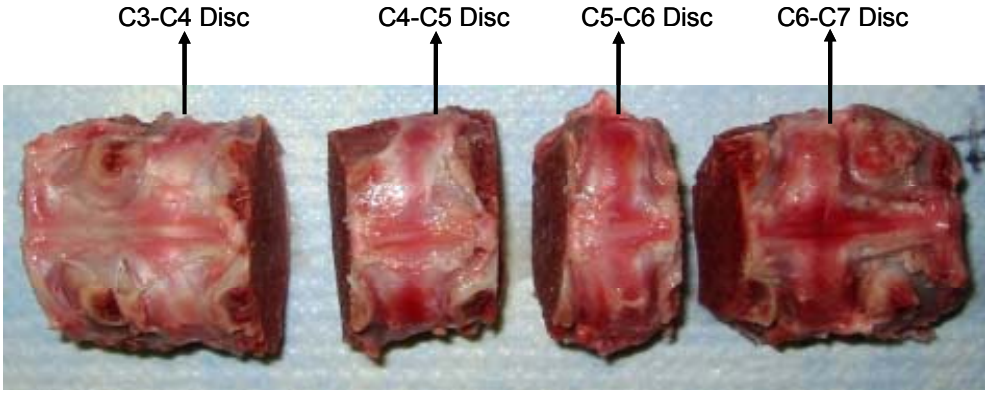

Figure 3.1. Posterior view of a cervical porcine spine, the posterior arch was removed and the vertebral bodies were cut transversally.

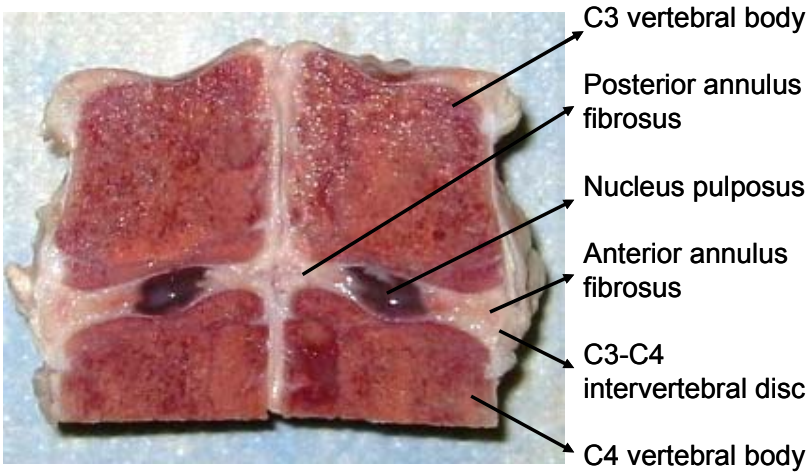

Figure 3.2. The C3-C4 vertebral bodies of the functional spinal unit were cut midsagitally from anterior to posterior into two blocks. The neurological arches were removed for macroscopic and microscopic dissection.

3.2 Summary Study 2.

Sixteen fresh frozen functional spine units were fixed in aluminum cups using a non-exothermic dental stone and steel wire. The mounted specimens were then placed in a dual axis servo-hydraulic dynamic testing system. Repetitive flexion–extension motions combined with 1472 N of compression were applied to the specimens. The experimental apparatus design has been detailed in Callaghan et al. (2001). A radio-opaque/dye mixture was injected into the disc to enable radiographic and visual tracking of the nucleus. The functional spine units (FSU) were tested in a range from 4400 to 14400 cycles of repetitive flexion of 15 degree and extension of 2 degree motion, then X-rays were taken and discography was performed. Dissection procedures and histochemical staining techniques were performed as described in Study 1, and the added radio-opaque/dye mixture can be seen (Figure 3.3). The histochemical staining technique was applied to characterize the presence of disc herniation.

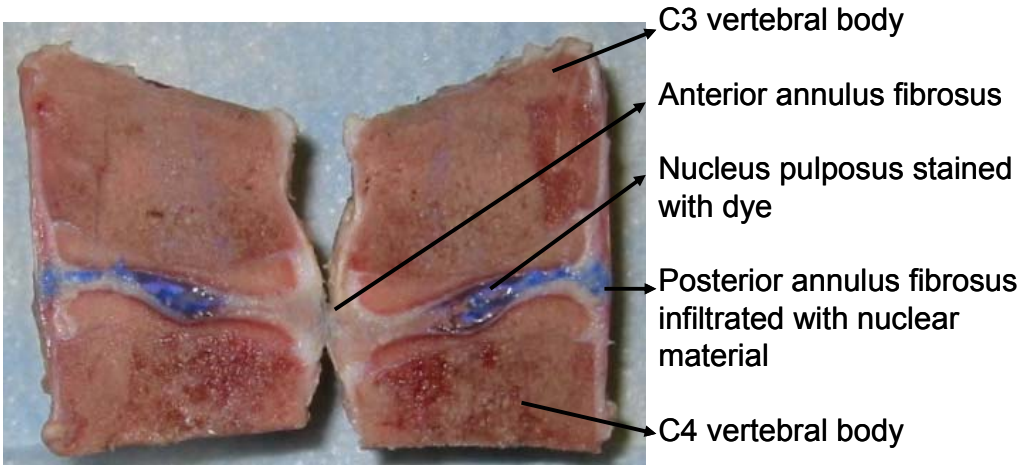

Figure 3.3. The C3-C4 vertebral bodies of the functional spinal units were cut midsagitally from anterior to posterior into two blocks after repetitive testing. The neurological arches were removed for macroscopic and microscopic dissection.

Study 1

3.1.1- Specimen Characteristics and Preparation

In the first study three fresh-frozen porcine cervical vertebral spine were prepared from C3 to C7, the neurological arch was removed with a saw and each vertebral body was cut across the middle of the vertebra in the transverse plane to divide them into two modified functional spine units; C3-C4, C4-5, C5-C6, and C6-C7 (Figure 3.1). For the study of the annulus laminate structure, the vertebral bodies were cut anterior-posterior into right and left blocks (Figure 3.2). The right half side was used for histological analysis and the left half side was used for macroscopic dissection. The macroscopic dissection was performed with the use of surgical instruments and a stereomicroscope (Nikon, SMZ1000) as shown in Figure 3.4 A. The FSU was fixed with clamps and light traction, around 10 N was applied with elastic bands along the axis of the spine to facilitate the dissection and to standardize the shape of the annulus

for digital pictures. The different steps of dissection were registered with a digital camera (Nikon, Coolpix 5400) and the image were “JPG” format with a dimension of 2592 x 1944 pixels. All measurements of length must be based on a comparison between the object under scrutiny with something of known dimensions, or with a standardized, calibrated scale. A Nikon calibrated microscopic slide was used for this purpose. Because this micrometer scale could not viewed simultaneously with the specimen, an image of the micrometer was recorded by the digital camera system.

The thickness of anterior and posterior annulus fibrosus, the number of lamellae layers, the degree of inclination of the lamellae bundles, and the thickness of the lamellae were measured from digital images using GIMP 2 software (GNU Image Manipulation Program, 2.2.10).

The thickness of anterior and posterior AF was measured in millimeters from digital pictures. The pictures were taken from a sagittal view of the anterior and posterior annulus fibrosus with the use of surgical microscope. The middle part of the height of the AF was used for the measurement of the thickness and the narrower distance between the superior and inferior end plate was considered to be the height of the AF.

The number of layers of the anterior and posterior annulus fibrosus in twelve discs was counted with the use of microscope and histochemical staining. The external and middle annulus was considered for measurement. In the vicinity of the nucleus pulposus, the boundaries between lamellae became poorly defined and the lamellae gradually were replaced by nuclear material. There was no clear demarcation between

the annulus fibrosus and the nucleus pulposus, for this reason the inner lamellae could not be considered and a precise number of lamellae could not be determined.

The orientation of the lamellae bundle with respect to the vertical axis of the spine was studied after microsurgical dissection of the anterior and posterior AF. At least seven digital pictures from the outermost to the innermost layer were taken. With the use of microsurgical scissors two adjacent laminar bundles were clearly identified and photographed. The inclination angle of two adjacent layers defined the criss-cross angle.

The variations of annulus structure with circumferential and radial location were quantified and compared with the data quantifying the structure of human intervertebral disc that has been published in the literature (Marchand et al. 1990, Tsuji et al. 1993, Cassidy et al. 1989).

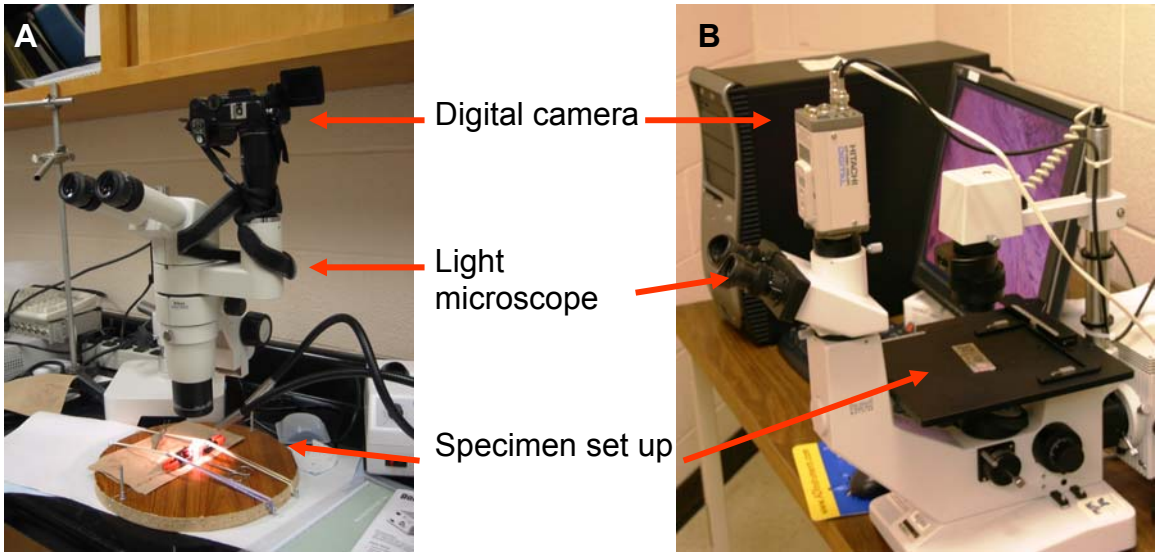

Figure 3.4. Light microscopes used for the analysis of the surgical dissections (A) and the stained slides (B).

3.1.2- Histology and Microscopic Description

The specimens for histology study were obtained from the right side of the disc. The sample of annulus was cut in blocks of 5mm height, 4mm width, and length depending on the part of the disc (anterior or posterior). The sample was embedded in gelatin, enveloped by Tissue-Tek OCT (Optimum Cutting Temperature; Miles Laboratories, Elkart, IN) compound. The block of tissue embedded in gelatin was rapidly frozen to -150 C° to -170 C° by immersion in liquid nitrogen, so that it hardened to a solid mass owing to freezing of tissue water. The anterior and posterior part of the disc were then sectioned transversely, sagittaly and in some case in 45 degree of inclination. The thickness of the slices was set at 10 micrometer. The samples were cut on a special microtome housed in a refrigerated cabinet (a cryostat) (Thermo, Electron Corporation). Cover slips treated with Vectabond® were used to increase the adhesiveness of the slice. In order to visualize detail and tissue structure at the light microscope level it was necessary to impart color to the slice. The sample was stained with haematoxylin and eosin for microscopy. A second light microscope (Hund, Wetzlar) connected to a digital camera was used to analyze the samples in the slides and digitize the microscopic images (Figure 3.4.B).

Study 2

3.2.1- Disc Herniation Creation Protocol by Callaghan and McGill (2001)

The cervical spines of 16 porcine (age mean six months, weight mean 785 N) specimens (C1-T12) were obtained immediately following death. All specimens were sealed in doubled polyethylene bags and stored at -22°C. Prior to testing, the frozen specimens were thawed at room temperature 24°C for 14 hours. The surrounding musculature was stripped leaving the osteoligamentous structures intact. Sixteen FSUs were obtained from C3-C4 (two adjacent vertebral bodies and the intervening intervertebral discs). The intervertebral discs of the sectioned ends of the specimens were examined for degeneration and were graded according to the scale proposed by Galante (1967). The sixteen specimens met the Grade 1 criteria and were chosen for the experiment.

The area of the exposed end plates (superior C3 and inferior C4) of the cervical porcine vertebrae was measured to evaluate resemblance in the size of the vertebral specimens as in the work of Callaghan and McGill (1995). The end plate area was calculated using the equation for surface area of an ellipse ($\pi/4*A*B$), where A is the anterior-posterior length and B is the medial-lateral width of the vertebral end plate, as in Figure 3.5. The average area of the two exposed end plates was used to represent the FSU area.

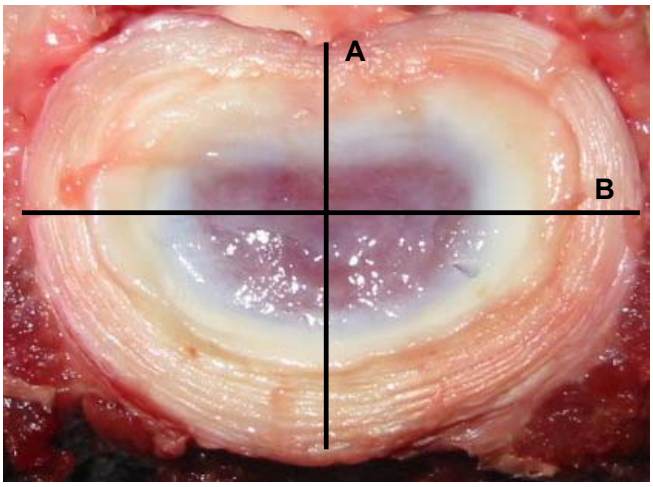

Figure 3.5. Intervertebral disc cut transversally shows how the end plate area was estimated from the anterior-posterior length (A) and the medial lateral width (B) using the equation Area= $\pi/4*A*B$.

To assist in the documentation of progressive tracking of the nucleus pulposus leading to intervertebral disc herniation, a mixture of barium sulphate (radio-opaque), blue dye (Coomassie Brilliant Blue Gmix: 0.25% dye, 2.5% MeOH, 97.25% distilled water), and distilled water was mixed in a ratio of 2:1:2 and approximately 0.7 ml was injected into the intervertebral disc nucleus with a 23 gauge needle. This mixture has sufficient resistance to diffusion over the duration of the test so that movement of the barium sulphate only occurs if a pressure is present. Specimens were then X-rayed prior to mounting in the testing machine to document the distribution of the nucleus in the sagittal and transverse planes. Specimens were fixed in aluminum cups using a non-exothermic dental stone (Denstone®, Miles, South Bend, IN, USA) and 16 gauge steel wire looped bilaterally around the anterior processes and the lamina of both vertebrae. Screws were also used to hold the specimen in the cup. The screws pierced the centre of the endplate and never protruded farther than 10 mm into the vertebral body. The dentalstone material only covered the proximal half of the cranial vertebra and the

distal half of the caudal vertebra. The mounted specimens were then placed in the testing machine (Figures. 3.6 (a) and 3.6(b)) as described in Callaghan et al. (2001).

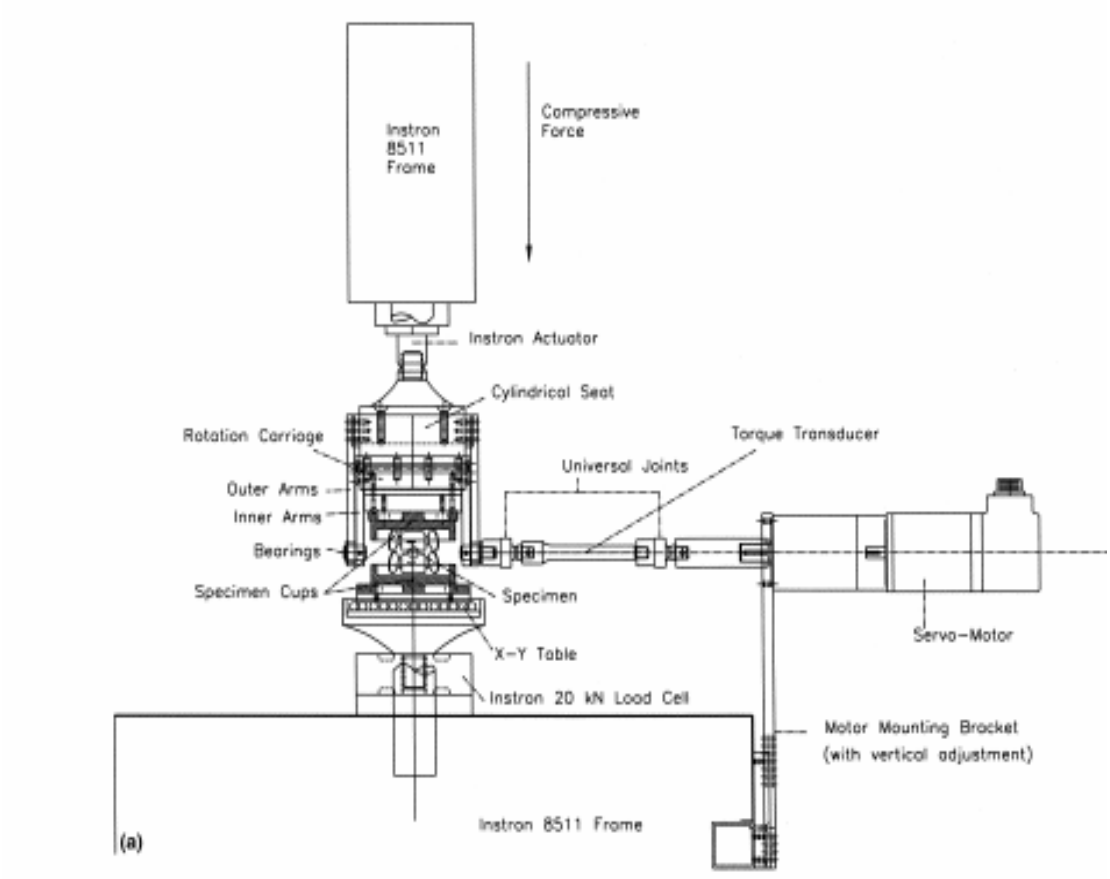

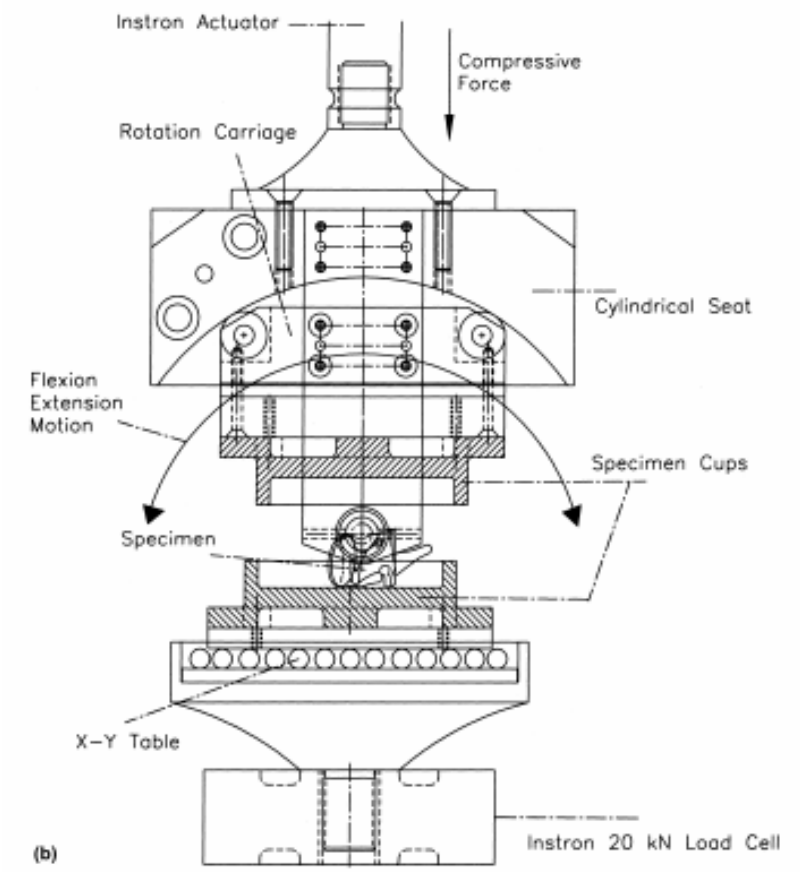

Figures 3.6. Frontal (a) and sagittal (b) view of the test apparatus used to apply coupled axial compressive load and pure flexion extension moments to produce repeated flexion extension motions. The X-Y table permitted translation to better represent in vivo conditions. (Callaghan, J.P., McGill, S.M., 2001. *Clinical Biomechanics*. 16, 28–37)

The testing jig was designed to allow the centre of rotation to be moved and aligned (vertically and horizontally) with the geometric centre of the intervertebral disc at the initiation of the test. The torques applied were applied as a pure moment in the sagittal plane. The specimens were free to translate in the horizontal plane (due to a ball bearing on the X-Y table mounted beneath the specimen) and freely rotate about the vertical axis, which allow the centre of rotation to move within the specimen during loading. This jig design has been previously shown to allow the specimens to deform

axially in response to the applied compressive loads and only compressive loads with flexion/extension moments were applied. To prevent drying from exposure to room air specimens were wrapped in two layers of a cotton fibre plastic backed material that had been soaked in a physiologic saline solution with an additional third plastic film wrapped around the specimen. Testing was conducted in a warm environment of approximately 26°C. A preload (260 N for 15 minutes) was applied to all specimens to counter any swelling that had occurred postmortem. During the preloading phase, the servomotor producing flexion/extension torques was set to zero and the angular position at the end of the preload was taken as zero position (elastic equilibrium) for each specimen. The specimens were then exposed to 1472 N of compressive load using the servo hydraulic dynamic testing system (Model 8511, Instron Canada, Burlington, Ontario, Canada). Previous work using the same test apparatus and specimen population has resulted in a documented compressive strength of 10.5 kN in a neutral posture (Gunning et al., 2001). The 1472 N compressive load represents approximately 14-22% of the average compressive strength of porcine cervical specimens reported in the literature (Aultman et al. 2004, Gunning et al. 2001, Parkinson et al. 2005). The flexion-extension range of motion was set at 15 degrees of flexion and 2 degrees of extension to maintain the applied torque to less than 35Nm. The overall average range of torque (maximum to minimum) applied across all of the specimens at the beginning of testing was 38.1 Nm ±12.6 and at the end of testing was 59.6 Nm ±13.6, so this approach yielded consistent loading of the specimens. Using these limits helped to preserve the disc tissue, avoided vertebral fracture, yet still produced herniations.

The specimens were then cyclically loaded in angular positional control at a rate of 1 Hz to a maximum of 14400 cycles and minimum of 4400 cycles using an electrical brushless servomotor (Model BNR3018D, Cleveland Machine Controls, Billerica, MA, USA) and a 40:1 planetary gear head (Model 34PL0400, Applied Motion Products, Watsonville, CA, USA)(Figure 3.7)

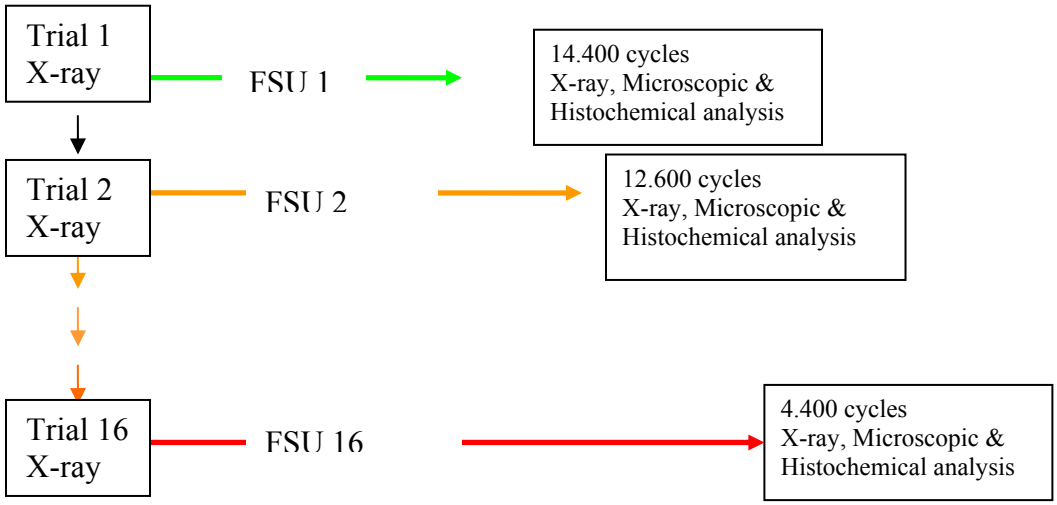

Figure 3.7. The experimental protocols used in Study 2 experiments are outlined. A total of 16 trials of 14400 to 4400 cycles were performed.

The servomotor was controlled using custom software which interfaced with an ISA bus motion controller (Model DMC1701, Galil Motion Control, Mountain View, CA, USA). Torque were measured using a strain gauge torque transducer (Model 01190-152, Sensor Developments, Lake Orion, MI, USA) and angular position data was obtained using an incremental optical encoder attached to the motor shaft (Model LDA-048-1000, SUMTAK Corporations of America, Piscataway, NJ, USA). The angular position, torque, axial force, and axial deformation were all A/D converted at a rate of 30 Hz for the full duration of each trial. The specimens were X-rayed

following testing in an attempt to track disc herniations to document both sagittal and transverse plane structures. A second injection of a mixture of barium sulphate and distilled water was then performed. Pressure on the syringe was increased slowly until the intrinsic disc pressure was exceeded. On average 1ml of the mixture was injected. A second discography was performed in attempt to increase the sensitivity of the X-ray method. A gross examination of the ligamentous structure and posterior elements was conducted and any failure or damage was recorded.

3.3- Statistical Analysis

3.3.1- Analysis of variance (ANOVA)

The angles of inclination for the different laminar layers, the thickness of individual lamellae, and the annular thickness and height were compared between the levels of the cervical spine (C3-C4, C4-C5 C5-C6, C6-C7) and between locations in the intervertebral disc (anterior and posterior annulus). A 3-way repeated measures ANOVA, (vertebral level, anterior/posterior IVD location, and laminar layer) was conducted to determine if the inclination angles were affected by the vertebral level in the spine and the location (anterior/posterior)in the disc, and /or the depth of the laminar layer (outermost-innermost). A 3-way repeated measures ANOVA (vertebral level, anterior/posterior, and external/middle locations) was performed on laminar layer thickness. Two-way repeated measures ANOVAs (vertebral level, and anterior/posterior location) were used to analyze the height and width of the anterior/posterior portions of the IVD. Rejection levels of 95% were used for all the ANOVAs. Duncan's post hoc multiples comparisons test were used to examine any

significant main effects, and least square means post hoc tests were used to examine any significant interaction effects.

4- Results

4.1- Measurements in First Study

Three fresh-frozen porcine cervical vertebral spines were sectioned from C3 to C7, the neurological arch was removed with a saw and each vertebral body was cut across the middle of the vertebra in the transverse plane to divide the spines into blocks; C3-C4, C4-5, C5-C6 and C6-C7. Twelve modified functional spine units were prepared for study.

4.1.1- Annulus Fibrosus Thickness

The thickness of anterior and posterior annulus fibrosus was measured in millimeters from digital pictures using GIMP 2 software. The pictures were taken from a sagittal view of the anterior and posterior AF. The middle part of the height of the AF was considered to perform the measurement of the thickness and the narrower distance between the superior and inferior end plate was considered to measure the height of the AF (Figure 4.1).

The average anterior annular thickness of 9.56 mm (± 0.84) was significantly larger than the average posterior thickness of 6.32 mm (± 1.76) (P=0.0001). The average annular height was not statistically different (P=0.108) between the anterior (6.31 mm ± 1.15) and posterior (5.57 mm ±0.83) compartments. There were no statistical differences between the different vertebral levels of the spine for annular thickness and height (P>0.888) (Table 4.1).

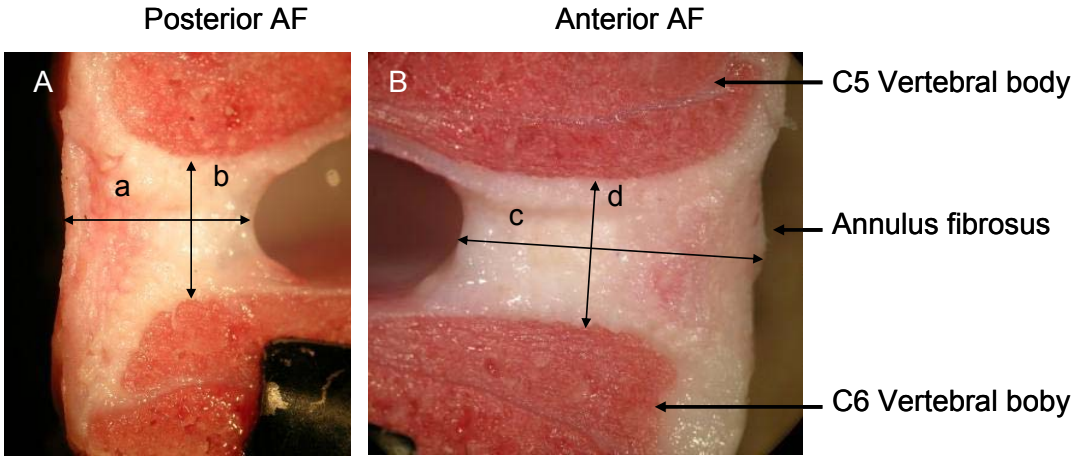

Figures 4.1. Sagittal view of a C5-C6 intervertebral disc measured from digital pictures with GIMP 2 software. Shown in A are the measurements taken from the posterior AF, for this specimen a=5.70 mm and b=4.94 mm. The measurements taken from the anterior AF are shown in B, and here c=10.10mm and d=4.88 mm.

Table 4.1. Measurements of the width and height in twelve cervical intervertebral discs.

	Anterior Annulus		Posterior Annulus	
Level	Width (mm)	Height (mm)	Width (mm)	Height (mm)
C3-C4 (n=3)	9.51 (± 0.71)	6.10 (± 1.68)	7.10 (± 1.21)	5.10 (± 0.51)
C4-C5 (n=3)	9.60 (± 1.34)	6.46 (± 1.16)	6.27 (± 2.22)	6.30 (± 0.98)
C5-C6 (n=3)	9.88 (± 0.52)	6.04 (± 1.03)	6.18 (± 2.46)	5.04 (± 0.13)
C6-C7 (n=3)	9.27 (± 1.03)	6.66 (± 1.07)	5.75 (± 1.53)	5.85 (± 0.86)
Overall				
C3-C7 (n=12)	9.56 (± 0.84)	6.31 (±1.15)	6.32 (±1.76)	5.57 (±0.83)

4.1.2- Number of Lamellae

The sample of annulus was cut in blocks of 5 mm height, 4 mm of width, and the length was dependant on the part of the disc (anterior or posterior) as shown in Figure 4.1. The annulus was cut into slices using a microtome in the transverse and sagittal directions, for histochemical staining. Some specimens were cut at inclination forty five degrees, parallel to the fiber bundles. This inclination allowed cutting some of the fiber bundles of the annulus in a transverse way and other in a longitudinal way. The fibroblasts are characterized by a large oval nucleus, a large nucleolus, and a tapering spindle-shape morphology. When the tissue was cut along the collagen fibers, these described shapes were easily identified (Figure 4.2). When the fibers are cut transversely, the tapered nucleus shape fades. The histological sample demonstrated clearly that fibers of one layer traveled in the opposite direction of the adjacent layer. The transverse and sagittal cut did not show a different shape.

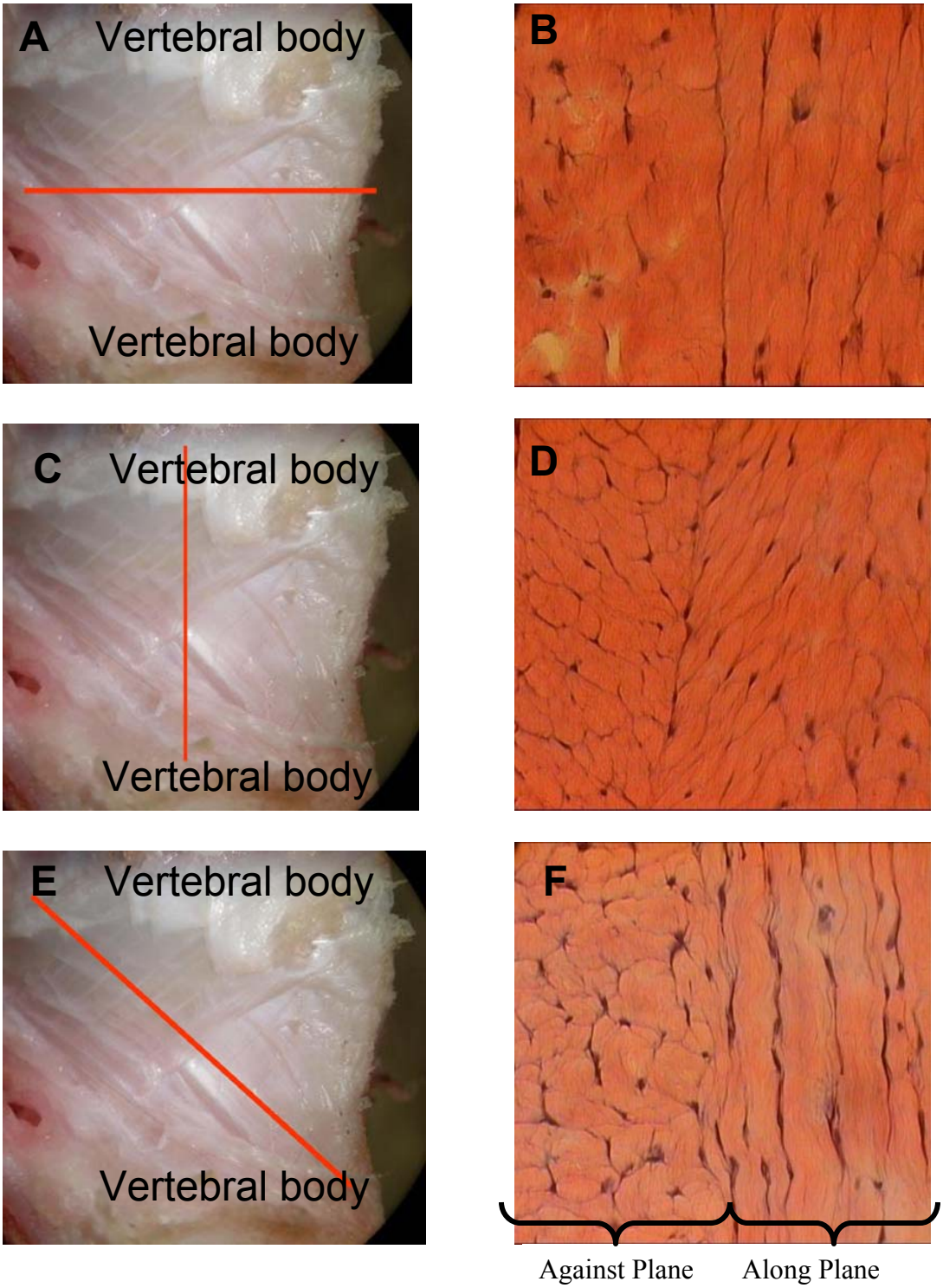

Figures 4.2. On the left side the transverse (A), sagittal (B), and longitudinal (E) planes along which the specimen was cut are illustrated. On right side, (B, D, F) two adjacent layers cut in the three different planes of inclination are shown (x40). The fibrocyte nuclei in two adjacent annular layers are oriented against and along longitudinal plane (F) respectively.

The number of layers of the anterior and posterior annulus fibrosus in twelve discs was counted with the use of microscope and histochemical staining. The external and middle annulus was considered for measurement. In the vicinity of the nucleus pulposus, the boundaries between lamellae became poorly defined and the lamellae gradually were replaced by nuclear material. There was no clear demarcation between the annulus fibrosus and the nucleus pulposus, for this reason the inner lamellae could not be considered and a precise number of lamellae can not be determined. The number of layers in the anterior annulus varied from 25 and 30 layers, compared to 18 to 20 layers in the posterior annulus.

4.1.3- Lamellae Thickness

The lamellae thickness of the anterior and posterior annulus fibrosus in twelve discs was measured with the use of microscope and histochemical staining. Digital images were used and GIMP 2 software was applied.

The thickness of each layer varied depending on the location within the anterior annulus. Two lamellae from the outermost and middle portions layer in the twelve discs were taken to quantify annular layer thickness. No measurements were taken of the innermost layer for reasons stated in Section 4.1.2. One lamellae chosen corresponded to the narrowest and the second to the widest lamellae from each of the external and middle area of the disc. The thickness of each of lamellae changed along the location of the anterior annulus. The outermost lamellae were narrow but generally the layers widened while approaching the nucleus (Figure 4.3).

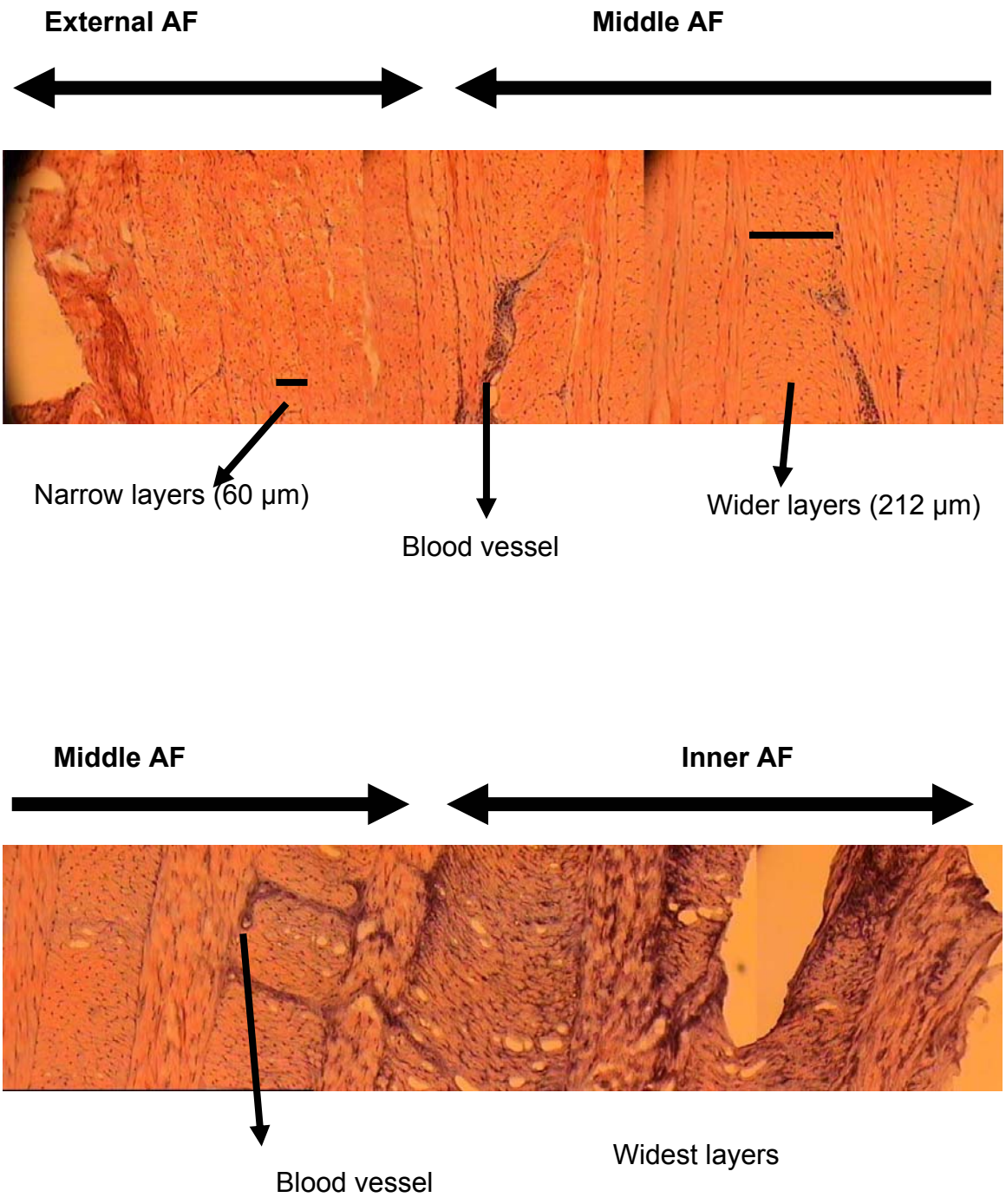

Figure 4.3. From images of the anterior annulus cut in a 45 degree inclination, magnified x10, and stained with H&E, show that the thickness of the lamellae increased as the nucleus pulposus was approached. Small vessels in the middle part of the annulus fibrosus are visible.

The thickness for the external layers in the anterior annulus ranged from a minimum of 0.028 mm to a maximum of 0.117 mm (average 0.079 mm, ±0.018) and for the anterior middle annulus ranged from 0.055 mm to 0.414 mm (average 0.192 mm, ±0.084).

The width for the outermost external layers of the posterior annulus ranged from a minimum of 0.023 mm to a maximum of 0.106 mm (average 0.062 mm, ±0.026) and for the middle posterior annulus ranged from 0.050 mm to 0.259 mm (average 0.134 mm, ±0.059).

The range (Figure 4.4) and the maximum measurements of annular thickness (Figure 4.5) had similar statistical outcomes. The range of maximum thickness for the external layers in the anterior and posterior annulus were not statistically different ($P>0.176$) but for the middle layer the anterior annular range in thickness was larger than the posterior ($P<0.014$). Both the anterior and posterior middle annular layer thickness range were larger than the external layers ($P<0.017$) (Figure 4.4). For the minimum annular layer thickness, both anterior external and the middle locations were significantly larger than the posterior and external location (Figure 4.6). No interaction effect of spinal level was found for any of the thickness measures ($P>0.304$, $P>0.057$).

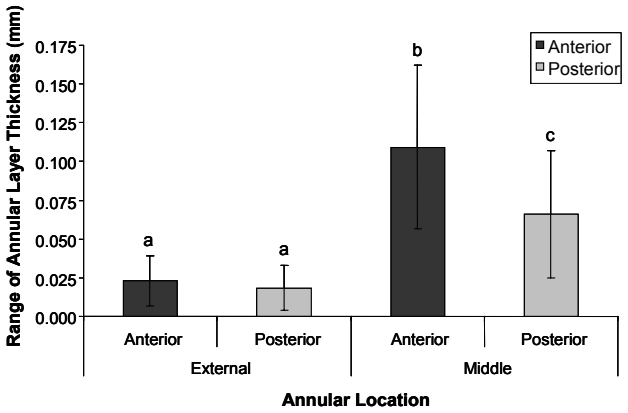

Figure 4.4. The range of layer thickness varied depending on the location within the external/middle of both the anterior and posterior of the IVD. Statistical differences between annular layers at different locations were found are indicated by different letters, with similarities marked by the same letter.

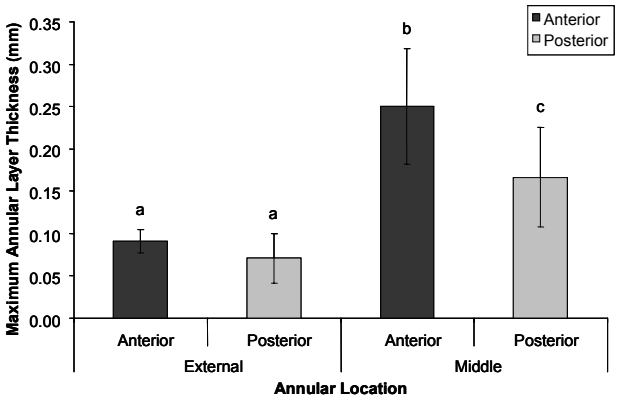

Figure 4.5. The maximum layer thickness varied depending on the location within the external/middle of both the anterior and posterior of the IVD. Statistical differences between annular layers at different locations were found are indicated by different letters, with similarities marked by the same letter.

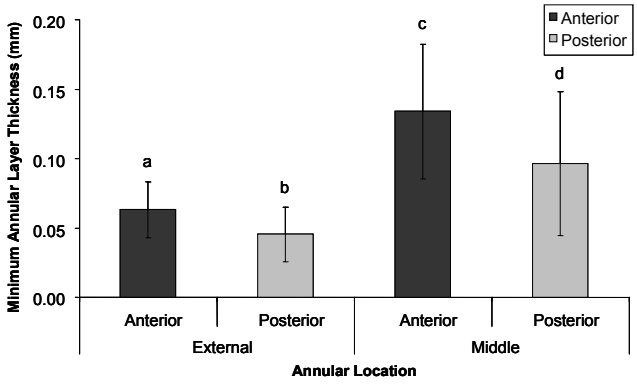

Figure 4.6. The minimum layer thickness varied depending on the location within the external/middle of both the anterior and posterior of the IVD. Statistical differences between annular layers at different locations were found are indicated by different letters, with similarities marked by the same letter.

In general the architecture of the annulus fibrosus was different comparing the anterior annulus with the posterior annulus from the porcine cervical spine. The results showed the posterior annulus is thinner, with fewer numbers of layers and narrower fiber bundles than the anterior annulus.

4.1.4- Blood Vessels and End Plate

The histological preparation showed small blood vessels over the outer and middle surface of the annulus. There were no branches in the inner annulus nor were there any in the nucleus pulposus (Figure 4.3). When the cartilage of the end plate was removed, in the subchondral bone small pockets of the marrow cavity against the surface of the end plate were observed (Figure 4.7.A-B) These pockets facilitate the diffusion of nutrients from blood vessels into the marrow space, and subsequently to the end plate and intervertebral disc.

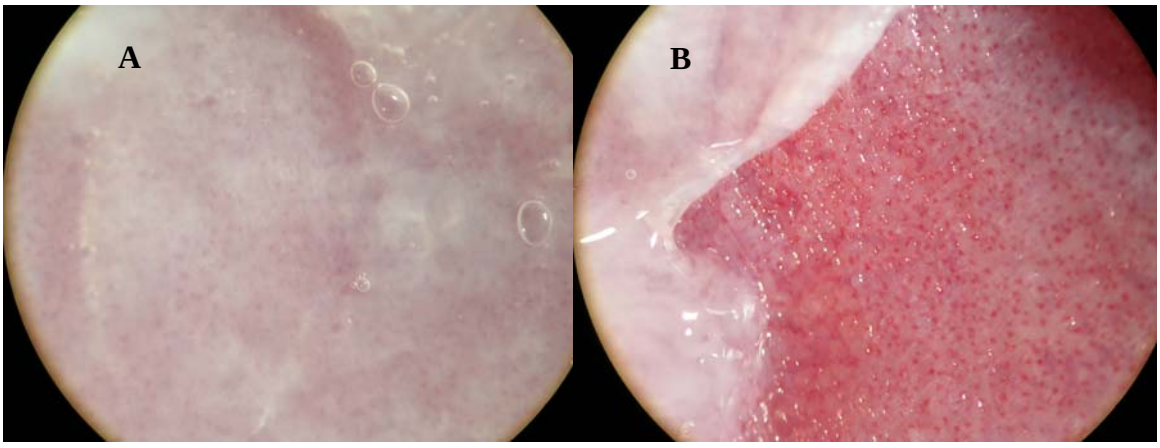

Figures 4.7. A) End plate of cervical porcine vertebra, microscopic view x2. B) End plate cartilage was removed to observe the porous surface of the subchondral bone.

4.1.5- Orientation of the Lamellae Fibers

The orientation of lamellae fibers with respect to the vertical axis of the spine was studied after microsurgical dissection of the anterior and posterior annulus. The technique allowed measuring the external, middle, and inner annulus. A least seven digital pictures from the outermost to the innermost layer were taken. With the use of microsurgical scissors two adjacent laminar bundles were clearly identified and photographed. The angle of the inclination between two adjacent layers defined the criss-cross angle (γ) (Figure 4.8). The angles of 14 different layers were measured from the outermost external layer to the innermost layer in the anterior and posterior annulus.

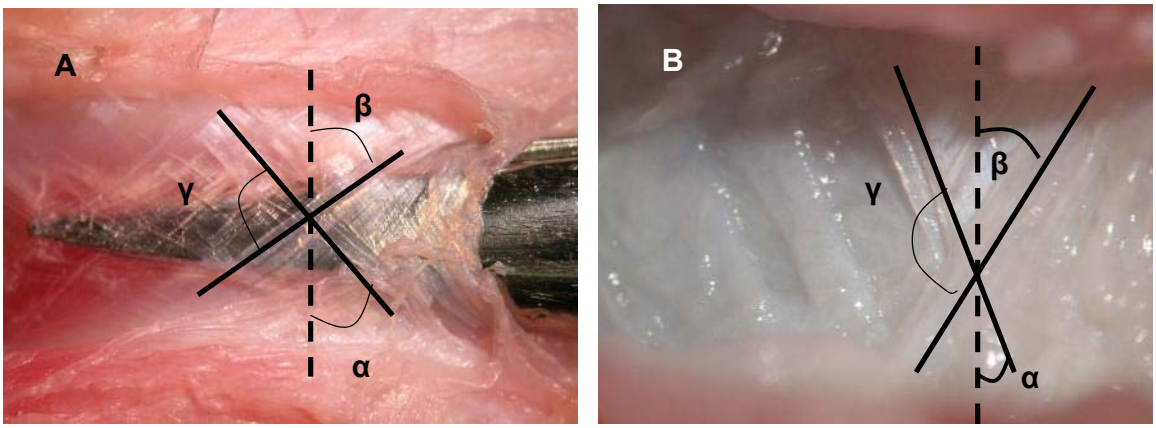

Figures 4.8. Dissection of the posterior C6-C7 AF. The posterior fiber angles were represented by α and β angle and the criss-cross angle by γ. A) α measured 42º and β measured 54º in the external layer and B) α measured 26º and β angle measured 32º in the posterior inner layer. The fibers become more vertical as the NP was approached.

The anterior AF from C3 to C7, showed an average inclination of 45 degrees (± 10.1) referred to the axis of spine, within 168 layers. Considering the first 10 layers as the external and middle annulus, the average inclination of the fibers was 48 degrees (±7.8, n= 120). In the last four layers (inner annulus), the average fiber inclination was

39 degrees (± 11.5, n=48). There was a significant increase in the bundle inclination ($P < 0.001$) where the inner bundles were more vertical relative to the external and middle bundles (Figure 4.9)

The posterior annulus showed an average inclination angle of 43 degrees (±10.9 n= 168). The 10 outermost layers, representing the external and middle annulus, had an average inclination of 46 degrees (±9.5, n=120). The fibers of the last 4 layers, representing the inner annulus, were on average 36 degrees (±11.8, n=48). There were no statistical differences in the angles of inclination when comparing the anterior and posterior annulus ($P= 0.116$) and no interaction between layer, anterior/posterior position or spine level ($P>0.396$). There was greater variability in the angle of the layers in the posterior annulus, but the decreasing trend from outermost to innermost layer was observed (Figure 4.10).

The orientation of the lamellae fibers were measured from two consecutive annular layers with respect to the vertical axis of the spine. The angle between two adjacent bundles is reported as the criss-cross inclination angle (Figure 4.11). Seven locations spanning from the outermost to innermost layers of both the anterior and posterior annulus were measured. The criss-cross inclination angle increased significantly from outermost to innermost locations ($P<0.0001$), but did not differ between anterior/posterior locations ($P=0.116$).

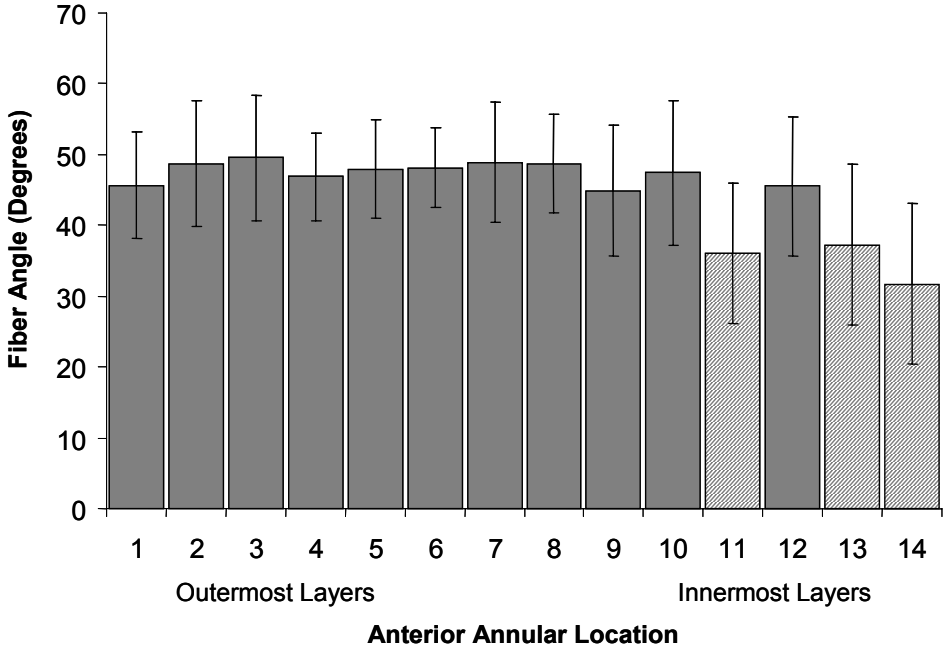

Figure 4.9. The anterior annular fiber inclination angle decreased from the outermost to the innermost layers of the annulus with respect to the vertical axis. The data is from two consecutive but oppositely running layers from seven locations spanning the anterior annulus. There was an interaction between anterior/posterior location and annular layer (p=0.034). Statistical differences between annular locations are indicated by different patterns.

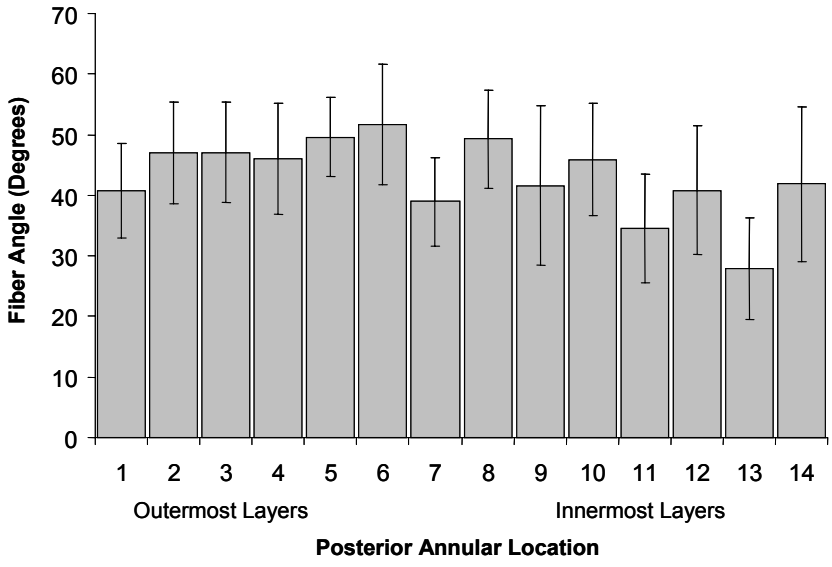

Figure 4.10. The posterior annular fiber inclination angle decreased from the outermost to the innermost layers of the annulus with respect to the vertical axis. The data is from two consecutive but oppositely running layers from seven locations spanning the posterior annulus. There was an interaction between anterior/posterior location and annular layer (p=0.034). Based on the least square means test, the data generally decreased from the outermost to the innermost layers, with the exceptions of layers 7 and 14.

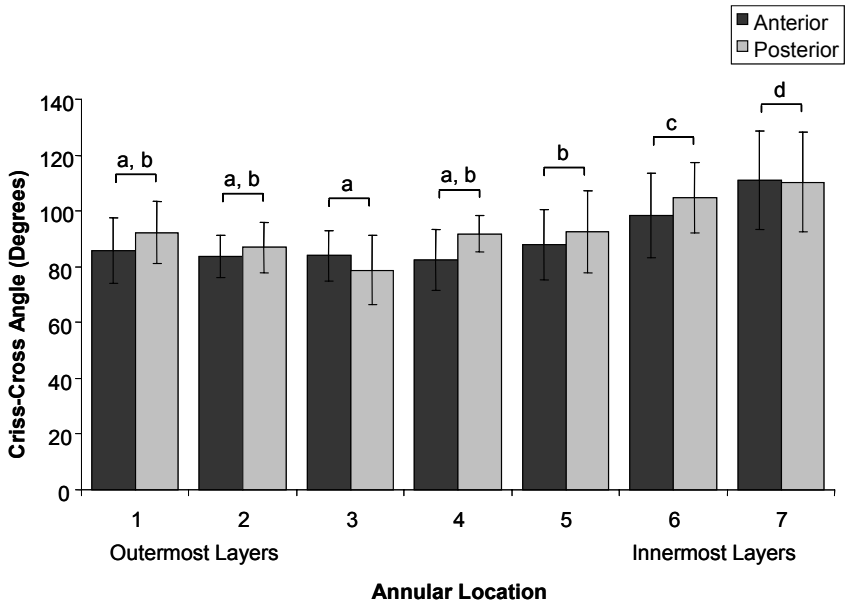

Figure 4.11. The criss-cross angle of the lamellae fibers pairs increased from the outermost to innermost layers of the annulus ($P<0.0001$). No statistical differences between anterior and posterior annular locations were found ($P=0.116$). Statistical differences between annular locations are indicated by different letters, and similarities by the same letter.

4.2- Measurements in Second Study:

Sixteen FSUs were used to study the mechanism of disc herniation. The damage was analyzed from the first inner layer of the annulus fibrosus to the outermost layers. The torque applied to the specimens to achieve the 15 of flexion and -2 of extension motion was similar regardless of the degree of damage that resulted (Table 4.2).

Table 4.2. The average range of torque applied (maximum – minimum) during the first 50 cycles of loading and the last 50 cycles of loading for the specimens is grouped by the three damage groups observed: no, partial, and complete herniation.

Range of Flexion-Extension Torque Applied to the Specimens

Damage Group	First 50 Cycles of Loading	Last 50 Cycles of Loading
No Herniation (n=4)	43.7 Nm (±19.9)	52.3 Nm (±24.1)
Partial Herniation (n=4)	42.8 Nm (±10.1)	62.4 Nm (±13.2)
Full Herniaton (n=8)	33.0 Nm (±8.2)	61.8 Nm (±6.0)

4.2.1- Disc Herniation Production

The aim of the experiment was to understand the mechanism of disc herniation by producing disc herniation from the initial signs of damage of the inner layer to the complete extrusion of the annular material. This study was not designed to be robust with large "n" for statistical analysis. The experiment produced eight complete herniations (Figures 4.1), four partial herniations and four specimens without any microscopic detectable annular damage.

In the 16 FSUs used, the average end plate area was 667.1 mm^2 ± 65.7 and ranged from 587.1 to 799.1 mm^2. There were no statistical differences between the end plate area, number of cycles applied and the occurrence of herniation (P>0.05) (Table 4.3) There was a specimen with complete herniation at 5400 cycles moreover there was another specimen without herniation at 8000 cycles with the same flexion-extension motion and torque. In two FSUs avulsion end plate fractures were produced in C4 at 7200 and 9000 cycles.

Table 4.3. The average end plate area and the average number of loading cycles applied for the three resultant groups of specimens: complete herniation, partial herniation and no detectable damage

Herniation level	End plate area (mm^2)	Number loading cycles applied
Complete (n=8)	657.8 (±64.3)	8700 (±3301)
Partial (n=4)	699.4 (±99.7)	5650 (±1226)
No detectable Damage (n=4)	653.4 (±9.84)	7550 (±2425)

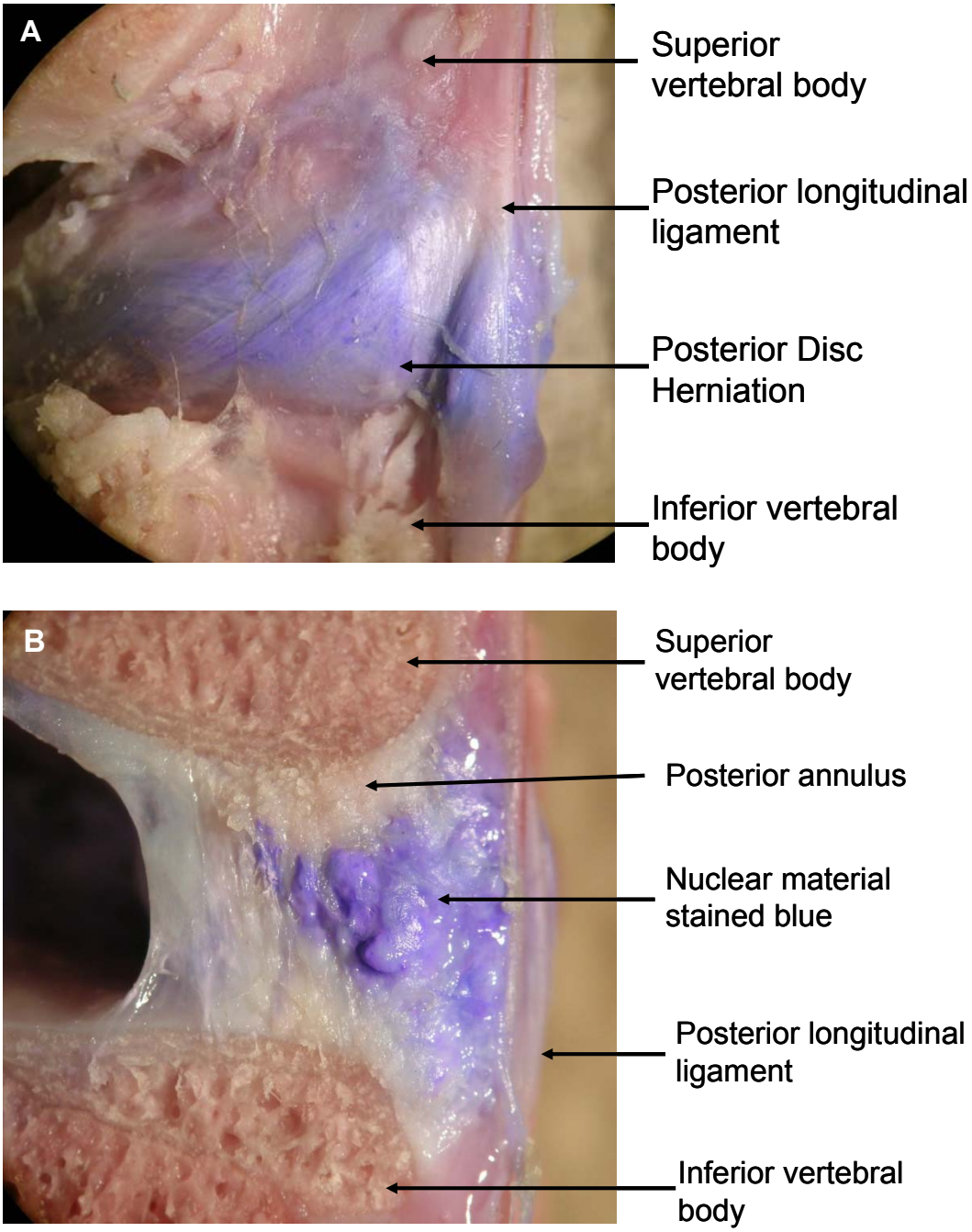

Figure 4.12. Complete disc herniation contained by the posterior longitudinal ligament, the nucleus was stained with blue dye. Shown from a posterior view (A) and sagittal view (B).

4.2.2 X-Ray Evaluation

Fourteen out of sixteen FSUs were X-rayed at the beginning and the end (Figure 4.13 A) of the trial to evaluate the tracking of the nucleus pulposus. (In two cases the X-ray machine malfunctioned, so no radiographic data was obtained). In eight specimens where the presence of complete disc herniation was defined by histochemical technique, four disc herniations were diagnosed by X-ray and three were misdiagnosed. In the four partial herniations only one could be diagnosed using X-ray technique. There were no false positives.

Once the experiment was finished, a second discography was performed in attempt to increase the sensitivity of the X-ray method (Figures 4.13, 4.14). There was no change in diagnosis of disc herniation and the additional mixture of barium was unable to show clefts or pathways where the nuclear material passed through the posterior annulus.

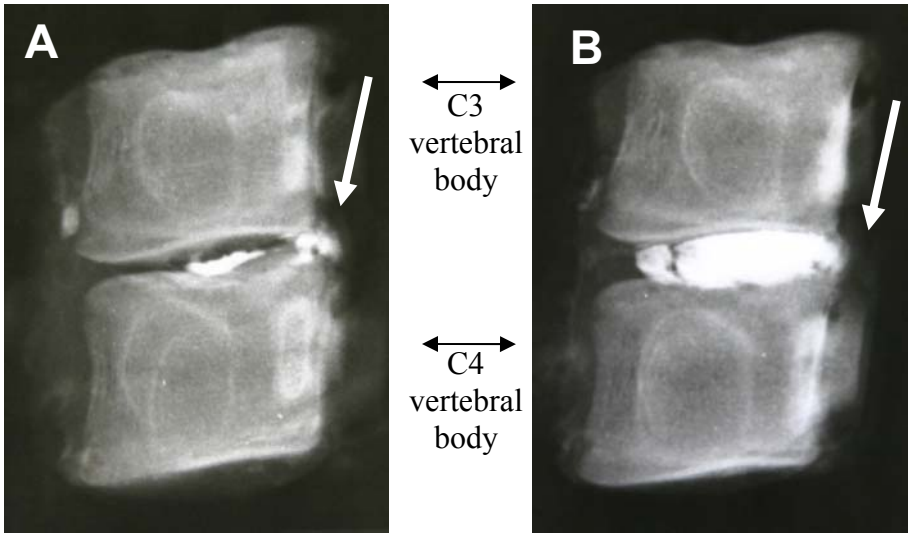

Figures 4.13. A C3-C4 FSU discogram post loading showed a posterior complete nuclear herniation (A) as indicated by the white arrows. A second discogram following an additional injection of radio-opaque showed no further leaking to the posterior vertebral canal (B).

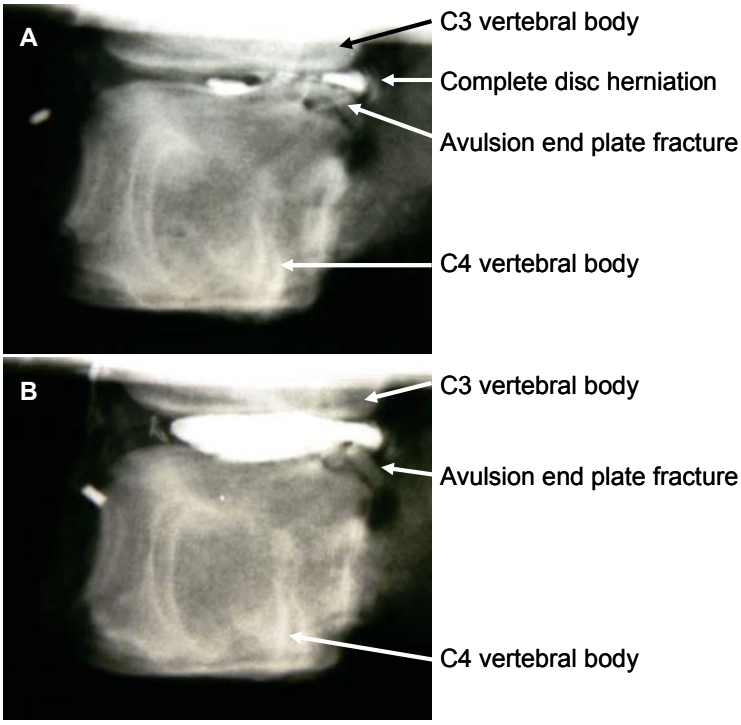

Figures 4.14. A C3-C4 FSU showed a complete posterior disc herniation and an end plate fracture after 9000 cycles (A). The injection of additional radio-opaque mixture was unable to show clefts or pathways where the nuclear material passed through the posterior annulus (B).

4.2.3- Micro-Dissection Analysis

Dissection was performed with the use of surgical instruments and a stereomicroscope to look for nuclear material in the posterior annulus. In eight specimens there was nuclear material reaching the posterior longitudinal ligament; therefore, these specimens were classified as complete herniations. In four specimens the nuclear material was between the inner layer and the middle layer; consequently, these specimens were classified as partial herniations. There was no nuclear material found in the anterior annulus. Nuclear material was found inside the lamellae bundles and filled in the direction of the fibers (Figures 4.15, 4.16). In one specimen the nuclear material reached the lateral annulus (Figure 4.17).

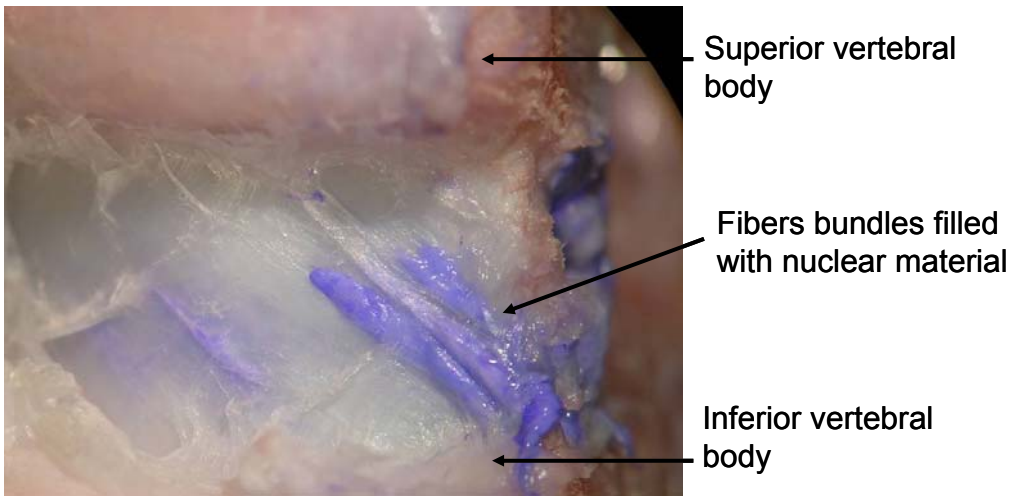

Figure 4.15. The nuclear material (stained blue) filled the fiber bundles of the posterior annulus fibrosus lamellae.

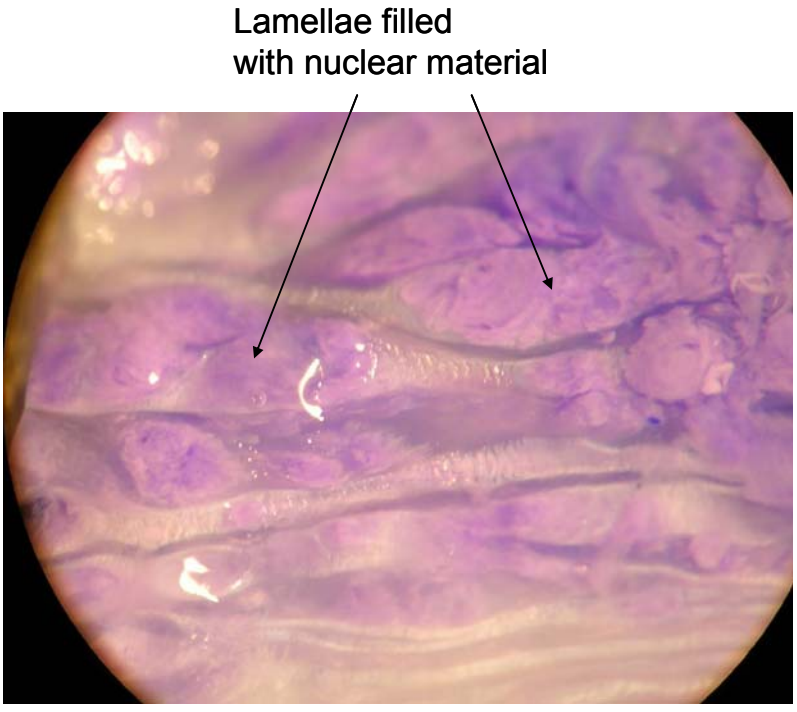

Figure 4.16. In a complete herniation, two adjacent lamellae were filled with nuclear stained material, the lamellae walls were preserved and a pocket of the nuclear material was created.

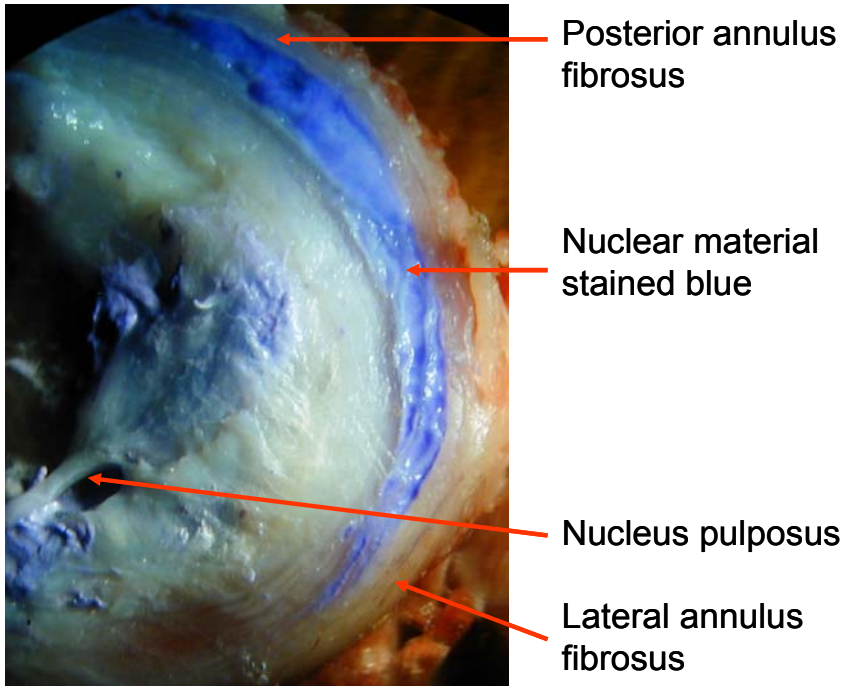

Figure 4.17. The IVD was cut transversally. The blue stained nuclear material can be seen to have extended from the posterior annulus to the lateral annulus in this partial herniation.

In six posterior annulus fibrosus, a small cleft was found connecting two adjacent layers lamellae. Nuclear material was found communicating from one layer to the other through the cleft (Figure 4.18, 4.19). There was a spreading of the fibers, and no rupture along the fiber was detected.

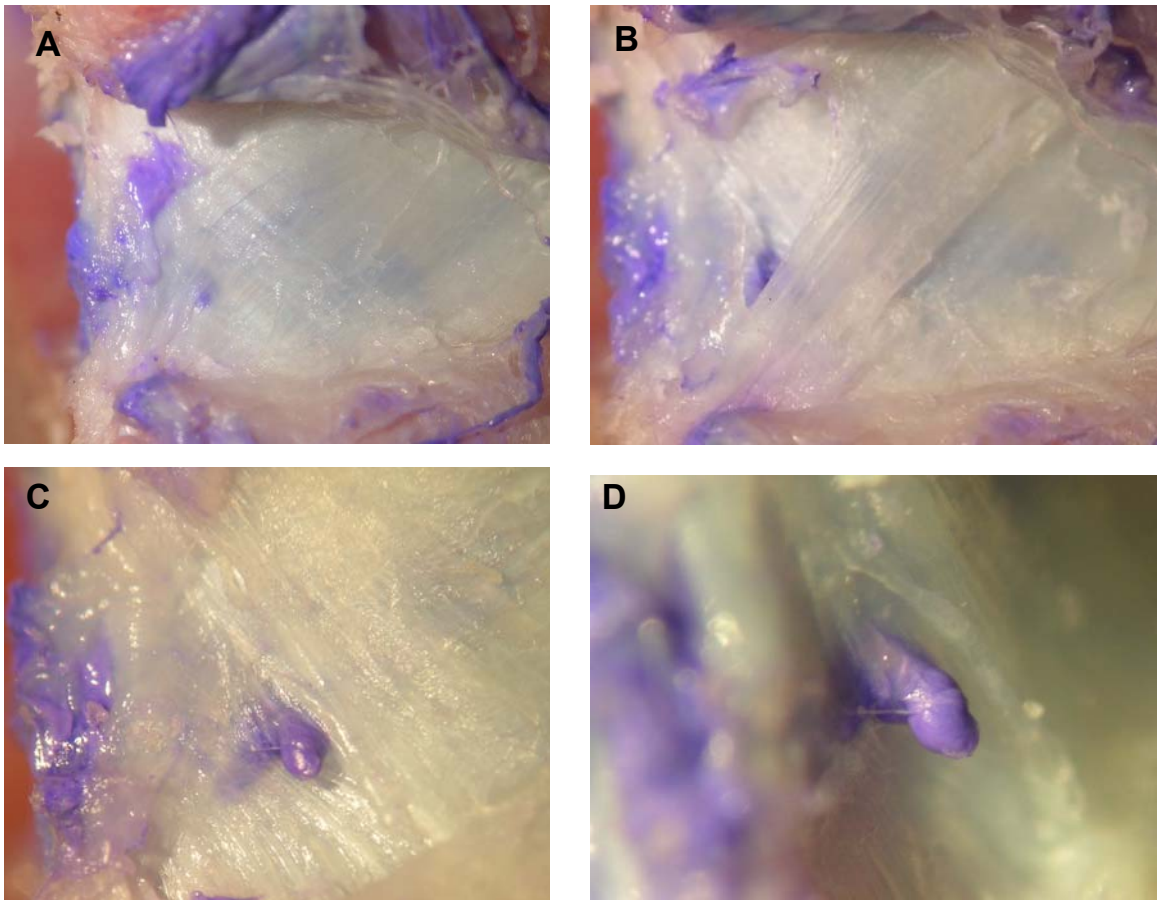

Figure 4.18. A dissection of the posterior annulus revealed where a small cleft had connected two adjacent lamellar layers and nuclear material that had passed through the bundles. The cleft is covered by a couple of lamellae (A). The adjacent lamellae were removed (B), and the cleft appears to have separated the lamellae bundles(C). The cleft and annular material in a lateral view (D).

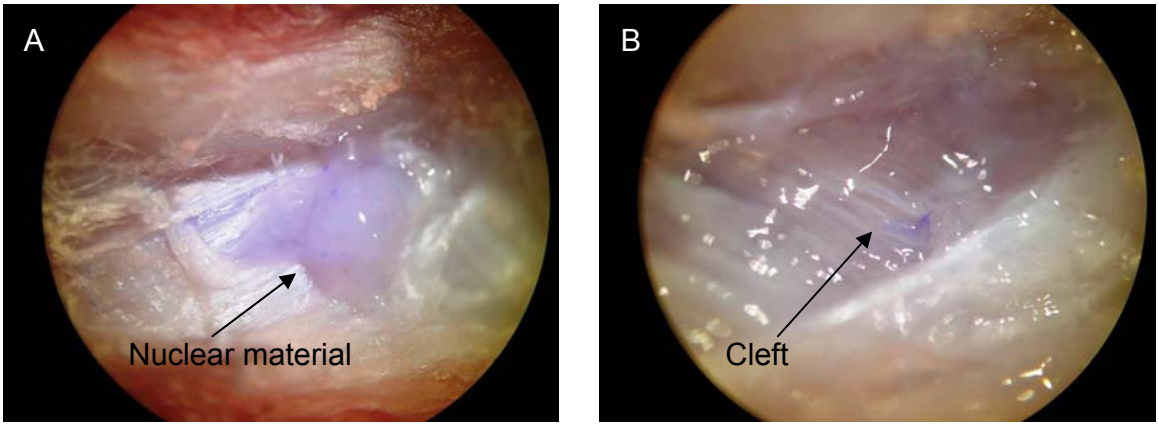

Figures 4.19. Dissection of the posterior annulus shows a partial herniation. The pocket was filled with stained nuclear material (A). A cleft spreads the fibers in the inner layer of the cavity (B).

4.2.5- Histological Analysis

Sixteen specimens for histology study were obtained from the right side of the disc. The samples of anterior and posterior annulus were cut in blocks, sliced in ten micrometer thick and stained with haematoxyline and eosin for microscopy. A light microscope connected to a digital camera was used to analyze the samples in the slides and digitize the microscopic images.

In four specimens there was no histological tissue damage in the anterior and posterior annulus. In four other specimens, nuclear material was found inside the lamellae bundles in the posterior annulus. The damage was characterized by the formation of a pocket filled with nuclear material, which has also been termed a cyst by Yasuma et al. (1986). In eight specimens nuclear material was found between the outermost external layer and the posterior longitudinal ligament. The lamellae structure in these eight cases was disrupted (Figures 4.20, 4.21).

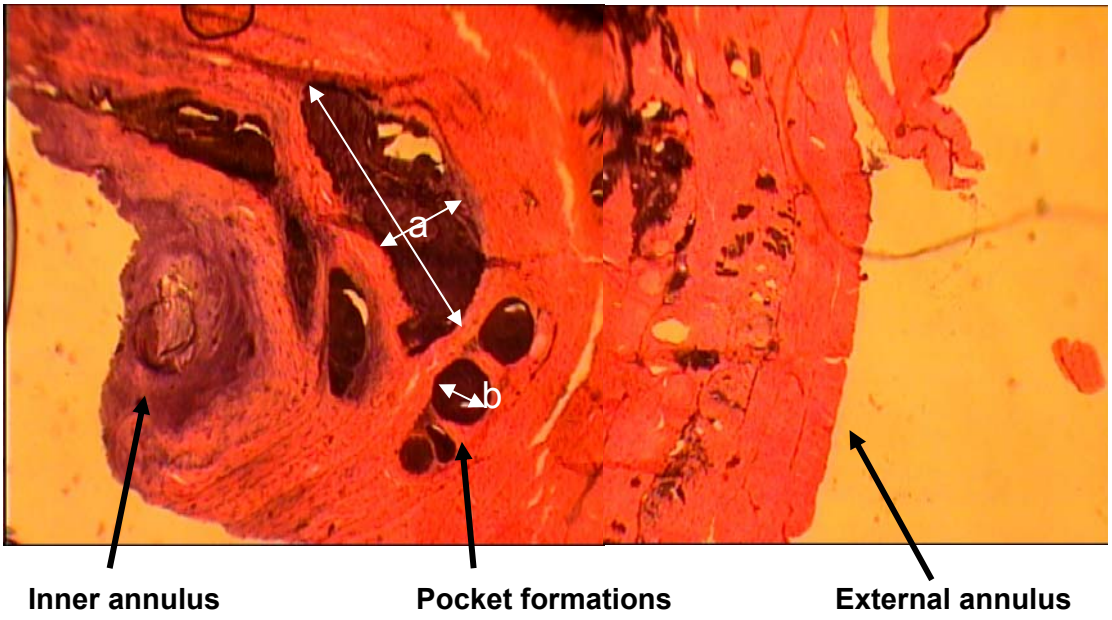

Figure 4.20. An image of the posterior annulus cut sagittaly, stained with H&E and magnified x4, shows pocket formations filled with nuclear material. Here pocket (a) measures 0.94 mm by 0.34 mm and (b) measures 0.22 mm.

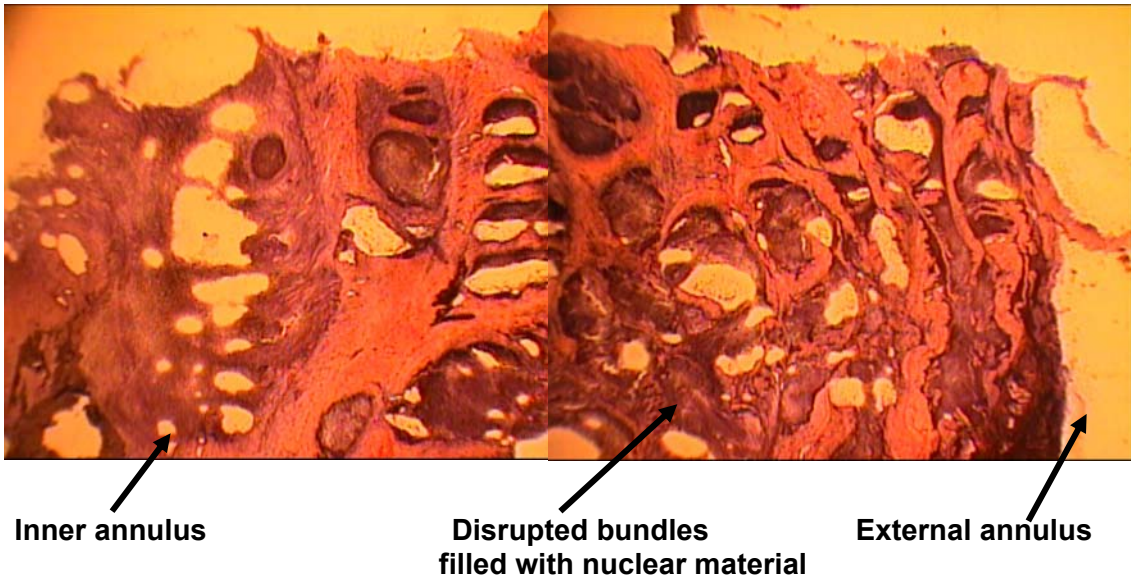

Figure 4.21. A histological sample of posterior annulus stained with H&E showing a complete disc herniation (magnification x4). The disruption of the lamellae by the nuclear material was produced after applying 7200 cycles of flexion-extension motions and low compressive load.

Figure 4.21 represents the most common feature of partial herniation, where the external lamellae presented no damage and the inner layers presented accumulation of nuclear material. The nuclear material filled the layer within the collagen fibers but not between the lamellae.

5-Discussion

5.1- Discussion First Study

The objective of this study was to assess the appropriateness of the porcine cervical spine model for the lumbar human spine. The structure of the cervical porcine disc resembled the lumbar human disc and appears to be suitable as a model. Small differences in the size and number of lamellae were evident. The size of the annulus was smaller, the thickness of the lamellae was narrower, and the number of layers was fewer. Studies have shown the porcine spine has anatomical (Oxland et al., 1991), geometrical and functional (Yingling et al., 1999) characteristics similar to the human lumbar spine. This thesis adds that the porcine intervertebral disc also has macroscopic and microscopic similarities to the lumbar human spine. The configuration of the disc tissues of the porcine specimens fall in the low range of human values reported in the literature. Consequently, the cervical porcine disc appears to be a slightly smaller scaled version of lumbar human disc. Therefore, the first hypothesis is accepted.

The first study analyzed the structure of the normal annulus fibrosus from cervical porcine discs. The intervertebral disc consists of three different structures: the nucleus pulposus surrounded by a peripheral annulus fibrosus, and the end plates, which cover the top and the bottom aspects of each disc. In our model, there were approximately 30 layers in the anterior annulus and approximately 20 layers in the posterior-lateral annulus, using histological preparations (Figure 5.1). Marchand and Ahmed (1990) performed a detailed investigation of the structure of the lumbar disc annulus fibrosus using a layer by layer technique and microscopic examination of various cut surfaces in both young and old specimens. They found the annulus, excluding the transition zone,

consisted of 15 to 25 distinct layers, depending on the circumferential location, the spinal level, and the specimen's age. Cassidy et al., (1989) studied the structure of the lumbar intervertebral disc with an optical microscope technique and found about 38 layers in the anterior annulus, excluding the inner layers.

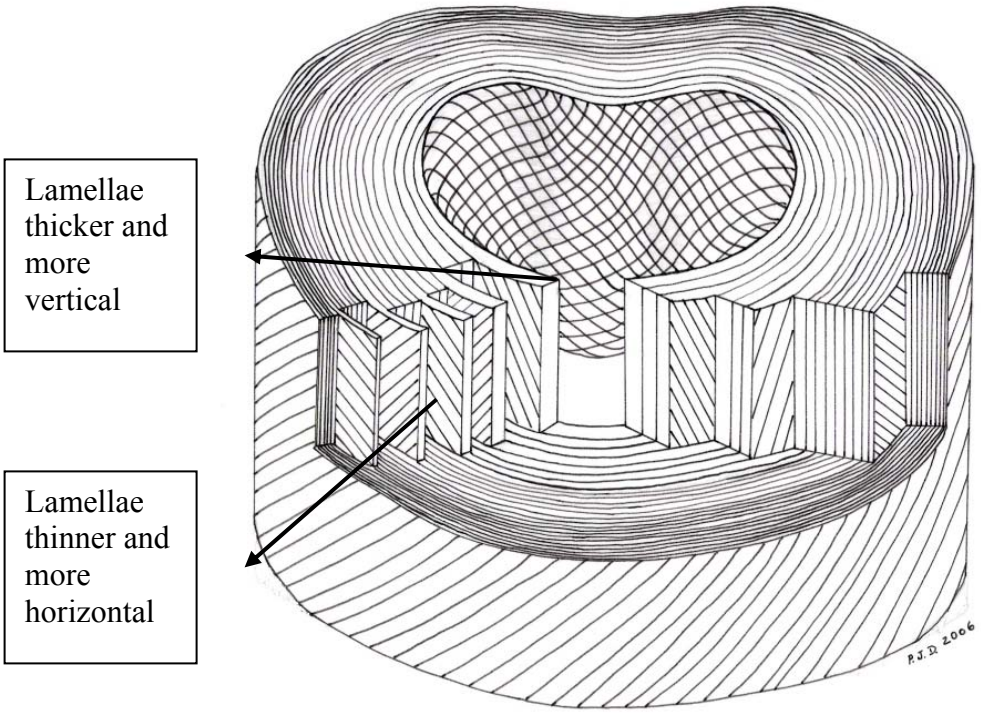

Figure 5.1. The detailed structure of the annulus fibrosus. Collagen fibers are arranged in about 30 concentric lamellae in the anterior annulus and about 18 in the posterior annulus. The orientation of fibers alternate in successive lamellae and there inclination and thickness increase approaching the nucleus pulposus.

The average width of lamellae increased from the outermost layer to the innermost layer from 0.062 mm to 0.192 mm. This pattern is similar in both the anterior and posterior-lateral annulus. A significant increase in the layer thickness occurred with decreasing proximity to the center of the disc. The posterior annulus was found to be thinner than the anterior because there were fewer layers and the thickness of each

bundle was on average narrower. In the human lumbar spine, the average layer thickness of young discs varies from 0.140 mm near the periphery to 0.200 mm near the center of the disc (Marchand et al., 1990). Cassidy et al. (1989) found that the thickness of the lamellae varied with radial location in the anterior annulus fibrosus. At the periphery of the disc, lamellae averaged approximately 0.130 mm. At the very edge of the disc, many lamellae less than 0.100 mm in thickness were found. This region extended from the edge of the disc inwards for 2.2 mm and represented the outermost 18 lamellae. At this point, there was a sharp increase in lamellar thickness to approximately 0.260 mm. In the posterior annulus they also found that the lamellar thickness was scattered and thinner, ranging from 0.050 mm to 0.250 mm with an average thickness of 0.135 mm. It could be functional to have the outer annular layers thinner as these are the portions of the disc that attach to the bony rim of the superior/inferior vertebrae and end plates.

The inner annulus contains both types of collagen, but mainly type II collagen which occurs in hyaline cartilage. The outer lamellae of both human and pig disc contain appreciable proportions of type I, but not type II collagen, which occurs predominantly in tendon and fibrous cartilage (Beard et al., 1980). In the histological preparations, type I collagen stained blue and type II collagen stained pink, which is the same feature as in human intervertebral disc.

Fiber orientation is remarkably important to understand disc mechanical properties. The change in fiber angles through the annulus may explain the mechanical function of the annulus fibrosus. Each lamella contains parallel collagen fibers which are tilted with respect to the spinal axis direction; the direction of tilt alternates from

one lamella to the next. The interlamellar angle was not constant through the thickness of the annulus. (Figures 4.5, 4.6, A-B). This pattern of tilted fibers can be observed by dissection of the disc. In this model the inclination angle averaged 48° in the external and middle annulus and 39° in the inner layers. Hsu et al., (1999) performed diffusion tensor microscopy in anterior lumbar porcine disc and showed alternating inclination angle approximately 30° to 50°. Studies with human spines have shown that the annular fibers are tilted by about 60° to 70° with respect to the spinal axis direction (Marchand et al., 1990, Bogduk et al., 1991, Adams et al., 2002). The inclination of the fiber bundles were scattered and varied from 0° to 90°. Cassidy et al., (1989) found in the posterior-lateral portion of the annulus, the angle of fiber orientation decreased from 62° at external annulus to 47° close to the nucleus. Guerin et al., (2006) studied the reorientation of the fiber structure when the intervertebral disc was loaded in compression or bending. They found the annulus fibrosus fibers reoriented toward the loading direction, with an average 17° decrease in fiber angle for non-degenerated tissue and 9.5° for degenerated tissue over 10% strain. They stated that these large changes in fiber angle indicate that fiber reorientation may significantly influence intervertebral disc mechanical behavior.

Human and porcine models share the same pattern in annulus fiber orientation however the porcine model presents a more vertical fiber angle. Similarities between young human intervertebral lumbar discs and porcine intervertebral cervical discs are summarized in Table 5.1.

Table 5.1. Similarities between young human intervertebral lumbar discs and porcine intervertebral cervical discs.

Features	Young Human Lumbar Intervertebral Disc	Young Porcine Cervical Intervertebral Disc
Number of layers	20 – 40 (*)	18- 30
Width of layers	0.059 mm -0.260mm (◊)	0.062 mm -0.192 mm
Tilted angle layer	47°- 62°(μ)	39° - 48°
Layer thickness	↑ outermost to innermost (†)	↑ outermost to innermost
Type of collagen	Type II in nucleus Type I in the annulus (‡)	Type II in nucleus Type I in the annulus
Type of cells	Fibrocytes and chondrocytes (ª)	Fibrocytes and chondrocytes
Small blood vessels	Peripheral layers (€)	Peripheral and middle layers
Inclination fiber angle	Inner more vertical (§)	Inner more vertical

(*) (Ghosh, 1988, Cassidy,1989, Marchand,1990), (◊) (Cassidy,1989, Marchand,1990), (μ) (Hsu, 1999 Bogduk,1991), (†) (Marchand, 1991), (‡) (Beard, 1980), (ª) (Ross, 1989), (€) (Bogduk,1991), (§) (Cassidy, 1989)

The structural characteristics of the cervical porcine annulus are represented in Figure 5.1. The posterior annulus is thinner than the anterior annulus, the number of layers in the posterior are fewer and thinner, and the thickness of the lamellae present the same pattern; thinner in the external edge with layers becoming thicker in the inner annulus. The inclination angle of the fibers show a decrease in the inner layer, and with the same pattern in the anterior and posterior annulus. Consequently, the first

hypothesis where the structure of the porcine cervical spine resembles the human lumbar spine, was confirmed.

5.2-Discussion second study

It was hypothesized that highly repetitive flexion-extension motions with relatively low magnitudes of compressive forces first produced a radial cleft in the annulus fibrosus, then disc delamination where the nucleus pulposus would be displaced and would accumulate, and finally if enough loading was applied a nuclear extrusion would result. However, a cleft was not observed to form through the annulus fibrosus as a straight path made by the nucleus pulposus. The nucleus was propogated through the annulus on a layer-by-layer basis, with intralaminar spreading (delamination) occurring after the nucleus had passed through the layer. The within layer delamination appeared to be due to hydraulic stresses from nuclear liquids rather than from applied motions and loads.

To relate the degree of damage to the cumulative loading variables (number of cycles, cumulative load applied, and time exposed), X-rays of the specimens at pre-specified intervals (i.e. every 1000 cycles) would have had to have been incorporated into the testing protocol. Upon detection of a predetermined amount of damage the loading protocol would have been terminated. Then the relationship between the loading variables and the degree of damage could have been investigated. The systematic tracking of damage was not performed in this study to maximize the integrity of the tissues for histological analyses by minimizing the overall testing time. As it turned out, without the systematic X-raying it was very difficult to “catch” a

partial herniation rather a complete herniation. However, this study was not designed to be a robust investigation of the mechanism of cumulative load injuries with a large number of specimens for statistical analyses. It was a histological based investigation of the mechanism of disc herniation. There are consistent results from previous studies that have linked herniation with cyclic motion, namely repeated flexion-extension motions with moderate compressive loads (Adams et al. 1985, Gordon et al. 1991,Callaghan et al. 2001). So while the methods in this study were not able to directly evaluate the second hypothesis, the loading protocol from proven cumulative load/cumulative injury model research (Callaghan et al. 2001) was used to produce the damage (herniation) that was quantified. Therefore, with this study using a small number of specimens, it is not possible to evaluate the second hypothesis but the results support the third hypothesis.

The use of direct puncture as a diagnostic procedure to study intervertebral discs began over forty years ago. Over the years, the development and improvements in imaging techniques, such as magnetic resonance imaging, have relegated the discogram to a provocative test more than an image diagnostic tool. However, correlation of symptoms with imaging data may not be sufficiently reliable to unequivocally determine the nature, location and extent of symptomatic pathology (Neuville, 1991). In the experiments, a mixture of X-ray contrast and blue dye was injected to track the nuclear material across the annulus. In four of seven specimens, the X-rays were able to show a complete posterior disc herniation, however the use of a second discogram did not increase the sensitivity of the diagnostic procedure. The kind

of annular damage sustained from the repetitive loading protocol did not allow the contrast fluid to penetrate easily and track a pathway (Figures 4.13, 4.14).

The histological compositions of herniated disc fragments have been investigated in many publications (Lipson, 1988, Mixter and Barr, 1934, Moore, et al., 1996, Yasuma et al., 1993). It seems clear that the method of nuclear material extrusion to the annulus fibrosus is different depending on the age of the subjects. Hard disc herniation occurs in older patients where fibrosis is present and pieces of cartilage of the end plate and new formation of small vessels are exhibited. Soft disc herniation is where the primary material found is nucleus pulposus (Willburger et al., 2004).

Yasuma et al. (1986) studied 257 intervertebral discs obtained at autopsy and disc material obtained from 441 operations for disc herniation, using histological techniques. They found slight fibrosis of the viscous matrix of the nucleus pulposus in sections from subjects who had died in the third decade of life or later. Myxomatous degeneration represented by cyst formation was seen in approximately 70 to 100 per cent of discs with complete extrusion or sequestration. The fiber bundles were separated and the cyst formations were inside the layer. The myxomatous degeneration is represented by aggregation of interstitial mucopolisacharid. Beatty (1985) found that in all sixteen patients that were operated for pain radiating into the sciatic nerve, when the annulus fibrosus was incised, soft, gray disc material extruded under pressure like toothpaste being squeezed from a tube. They qualified this syndrome of myxomatous degeneration as a distinct entity, different from classical fibrotic disc degeneration or herniated nucleus pulposus. Lee et al. (2000) studied histological specimens of 15 patients with lumbar disc herniation aged 14 to 19 years. Only in one case, was

adequate trauma reported. All patients exhibited degenerative changes of the disc, similar to those observed in adults like mucoid degeneration, fibrosis and the presence of cysts. Marked cyst formation was observed in 6 patients. Finally, Willburger et al. (2004) studied the possible correlation between histological composition of herniated lumbar disc fragments and pain, disability, clinical signs and operative findings in fifty-five patients. In patients less than 30 years of age, significantly higher percentages of nucleus pulposus were found than in the older group, whereas annulus fibrosus was found in significantly higher percentages in patient older than 30 years.

It is hypothesized that the flexion-extension motion combined with a low-level load produced an increased hydraulic pressure in the inner wall of the posterior annulus. This pressure first produced a small cleft, spreading the collagen bundles inside the first layer. The nuclear material was "pumped" through the small cleft to the first layer filling the layer creating a fluid-filled pocket between the collagen fibers (Figure 5.2). Once the pocket acquired enough pressure a new cleft was produced in the weakest part of the layer allowing the nuclear material to create a new cavity in the second layer. This was the first stage of damage and disc herniation production at a microscopic level. Once there was enough nuclear material and the pressure in the pocket achieved a certain value, a new cleft was produced allowing the nucleus to pass to the third layer. The accumulation of nuclear material increased successively from the inner layer to the more external layers, while the nucleus was traveling along the annulus (Figure 5.2). This mechanism was repeated until the nucleus traveled along the annulus reaching the posterior longitudinal ligament. At this point a complete extrusion herniation was produced. In all 12 damaged discs, NP-filled pockets were found in the

posterior annulus and no nuclear material was found between the lamellae. The relatively more vertical inclination angle of the inner lamellar layers is postulated to be the most resistant to NP penetration. As the layers become more horizontal, and subsequently more external, the layers are likely more easily parted, and so less capable of containing the nucleus pulposus.

The pocket produced by the nuclear material filled in the direction of the layer bundle fibers, creating a criss-cross pattern in two adjacent layers. The extension of the cavity depended on the extension of the bundle. In the middle annulus there were more horizontal bundles, with low inclination angle, that allowed the nuclear material to reach the lateral portion of the disc.

Delamination was defined in this study as the spreading of the collagen that occurred inside of the bundles, within the limits of a given layer (Figure 4.16). The shape of the delamination took the same inclination angle of the layer. Two adjacent delaminations, filled with nucleus, had the same criss-cross pattern as the lamellae bundles. The spreading of a layer was only observed after the nucleus had passed through the layer. In the partially herniated specimens, no delamination was observed in the layers external to those infiltrated by nuclear material. Therefore, the within layer delamination appeared to be due to hydraulic stresses from nuclear liquids rather than from applied motions and loads.

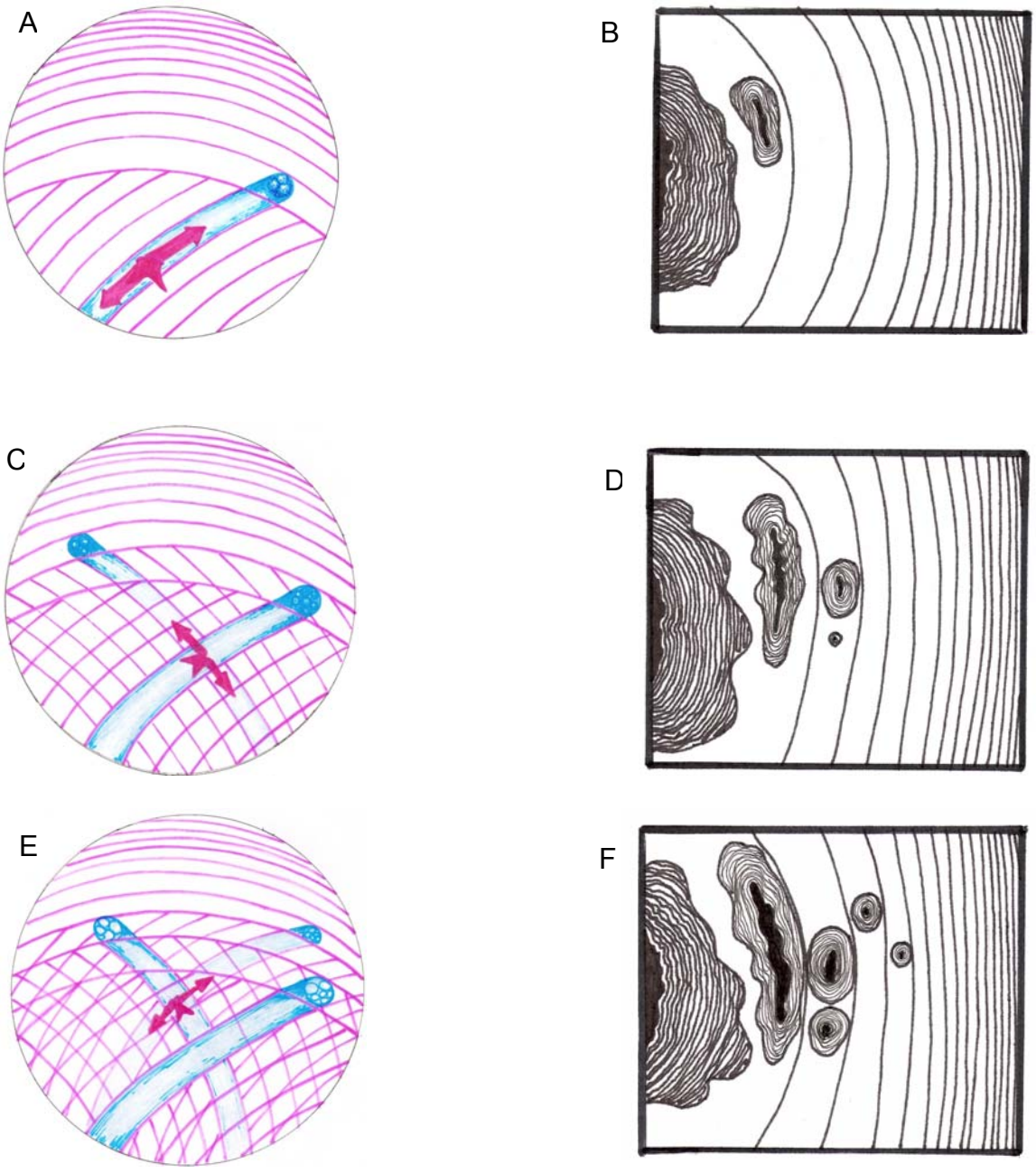

Figure 5.2. Schema of the proposed mechanism of disc herniation production.A,C,E) Oblique superior view from the inside to the outside of the IVD (A, C, E), and a transverse view are illustrated (B, D, F). A cleft is produced in the first layer by the pressure of nuclear material, from inside to outside the annulus fibrosus (A, B). Once the nuclear material reaches certain pressure a second cleft is produced and the second layer is filled with nuclear material (C, D). This mechanism is repeated and the nucleus travels along the annulus fibrosus producing a disc herniation (E, F).

There were no clefts or breaches in the lamellae that crossed two adjacent layers in a linear shape. The pathway of progression of the nuclear material was not linear. The clefts were created in the weakest part of the lamellae wall. Isolated clefts without nuclear material were not found in the anterior and posterior annulus. The formation of clefts was produced by combination of repetitive flexion extension motion and by the hydraulic pressure of the nucleus pulposus. In two cases a fatigued end plate fracture occurred, however, no detachments of insertion of the bundles were found.

The myxomatous degeneration reported as microscopic cysts in young human intervertebral discs could be produced by nuclear material and could represent the first stage of the mechanism of disc herniation creation (Figure 5.3).

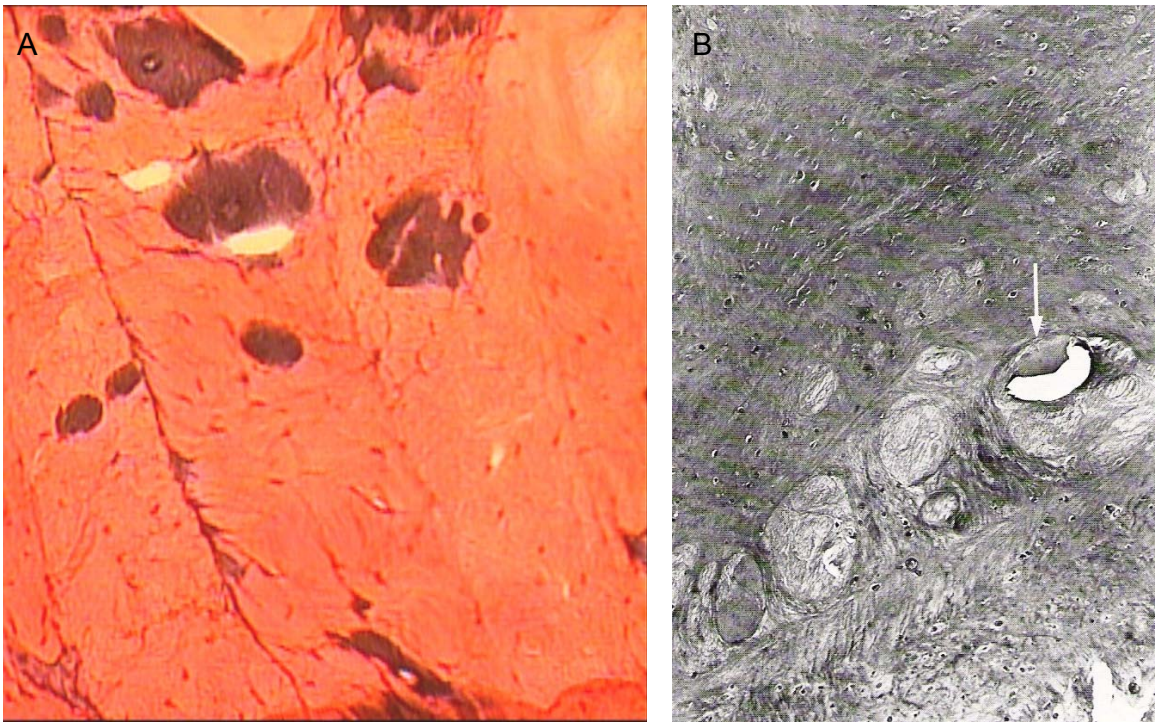

Figure 5.3. The annulus fibrosus showing (A) lamellar pocket formation found in porcine annulus (stained with H&E, x10) and (B) myxomatous degeneration with cyst formation (arrow) (stained using alcian blue with periodic acid-Schiff, x10). Yasuma et al.,1986. Histological development of intervertebral disc herniation. *The Journal of Bone and Joint Surgery* 68-A 1066-1072.

The classical disc herniation is composed of fibrotic material, which represents prolonged production of tissue damage. In this porcine model the mechanism of combined motion and load may replicate the mechanism of cumulative load in a young disc which possesses hydraulic behavior.

Consequently, these microscopic and macroscopic findings suggest herniation results from repetitive flexion-extension motions with compressive forces, and that the nucleus propogates through the annulus on a layer-by-layer basis. Intralaminar spreading rather than linear cleft formation follows the NP movement through the disc and appears to be due to hydraulic stresses from nuclear liquids. So while the methods in this study were not able to directly evaluate the second hypothesis, the loading protocol from proven cumulative load/cumulative injury model research (Callaghan et al. 2001) was used to produce the damage (herniation) that was quantified. Therefore, with this study using a small number of specimens, it is not possible to evaluate the second hypothesis but the results support the third hypothesis.

6. Conclusions

The structure of the cervical porcine disc resembles the lumbar human disc and appears to be suitable as a model to understand the mechanism of disc herniation when the spine is subjected to flexion extension motions combined with a low-level load. The cervical porcine disc appears to be a slightly smaller scaled version of the lumbar human disc

The highly repetitive flexion-extension motion combined with a low-level compressive load produced an increased hydraulic pressure in the inner wall of the posterior annulus. This pressure of the nucleus pulposus and motion of the specimen first produced a small cleft, spreading the collagen bundles inside the first layer which are the most resistant to nuclear penetration due to the vertical orientation of the fibres. The nuclear material was “pumped” through the small cleft to the first layer filling the layer creating a NP fluid-filled pocket. Once the pocket acquired enough pressure a new cleft was produced in the weakest part of the successive layer allowing the nuclear material to create a new pocket in the second layer. This was the first stage of damage and disc herniation production at a microscopic level. Once there was enough nuclear material and the pressure in the pocket achieved a certain value, a new cleft was produced allowing the nucleus to pass to the third layer. This mechanism was repeated until the nucleus traveled along the annulus reaching the posterior longitudinal ligament. Moreover, the microscopic findings in the porcine model are very similar to observations previously reported from young humans.

7. Limitations and Future Directions

7.1 Limitations

The main limitation of this work was to use the histological techniques to quantify the structures of the intact and damaged specimen samples. The steps involved to obtain a thin stained tissue sample included the dissection from the FSU, freezing, mounting, cutting, fixing to the slides, and staining. The cutting and staining procedures were the most deleterious on the tissue samples. The techniques resulted in some question regarding the degree of standardization among the tissue samples.

To improve the quality of the samples, it is suggested that the attachment of the disc to the endplate be preserved. This could help prevent the curving of the tissues during the cutting and staining procedures, improving the viability of each tissue sample for quantification.

7.2 Future Directions

It would be interesting to analyze whether the age of the porcine specimen could cause different variations in the mechanism of disc herniation compared to those documented in this work. An old pig would be a valuable tool for a new study. Injury mechanisms may be different for older spines due to the age related changes.

Another direction would be to evaluate if reverse loading (for example relatively large extension and small flexion motions) can reverse the process of disc herniation once already produced, and as a counter-movement to impede both the formation and progression of a herniation.

8-References

Adams, M.A., Hutton, W.C., 1985. Gradual disc prolapse. *Spine* 10, 524-531.

Adams, M.A., Bogduk, N., Burton, K., Dolan, P., 2002. The biomechanics of back pain. Churchill Livingstone, Toronto.

Allan, D.G., Russell, G.G., Moreau, M.J., Raso,V.J., Budney, D. 1990. Vertebral end-plate failure in porcine and bovine models of spinal fracture instrumentation. *Journal of Orthopaedic Research* 8, 154-156.

Aultman, C.D., Drake, J.D.M., Callaghan, J.P., McGill, S.M., 2004. The effect of static torsion on the compressive strength of the spine: an in vitro analysis using a porcine spine model. *Spine* 29, E304–E309.

Bancroft, J.D., Cook, H.C. 1984. Manual of histological techniques. Churchill Livingstone. New York.

Beard, E., Ryvar, R., Brown,R., Muir, H. 1980. Immunochemical localization of collagen types and proteoglycan in pig intervertebral discs. *Immunology* 41, 491-501.

Beatty, R.A. 1985. Myxomatous degeneration of the lumbar intervertebral disc. *Neurosurgery* 17, 277- 280.

Biering-Sørensen, F., 1983. A prospective study of low back pain in a general population. *Scandinavian Journal of Rehabilitation Medicine* 15, 71-79.

Bogduk, N., Twomey, L.T. 1991. Clinical Anatomy of the lumbar spine. Churchill Livingstone. New York.

Brinckmann, P., Biggemann, M., Hilweg, D. 1989. Prediction of the compressive strength of human lumbar vertebrae. *Clinical Biomechanics* 4 (Suppl 2).

Butler, W.F. 1988. Comparative anatomy and development of the mammalian disc. CRC Press, Boca Raton.

Cassidy, J.J., Hiltner, A., Baer, E. 1989. Hierarchical structure of the intervertebral disc. *Connective Tissue Research* 23, 75-88.

Callaghan J.P., McGill, S.M. 1995. Frozen storage increases the ultimate compressive load of porcine vertebrae. *Journal of Orthopaedic Research* 13, 809–812.

Callaghan, J.P., McGill, S.M., 2001. Intervertebral disc herniation: studies on a porcine model exposed to highly repetitive flexion/extension motion with compressive force. *Clinical Biomechanics* 16, 28–37.

Cassidy, J.J., Hiltener, A., Baer, E. 1989. Hierarchical structure of the intervertebral disc. *Connective Tissue Research* 23, 75-88.

Coventry, M.B., Ghormley, R.K., Kernohan, J.W., 1945. The intervertebral disc: Its microscopic anatomy and pathology-Part I. Anatomy, development and physiology. *The Journal of Bone and Joint Surgery* 27, 105-12.

Coventry, M.B., Ghormley, R.K., Kernohan, J.W. 1945. The intervertebral disc: Its microscopic anatomy and pathology-Part III. Pathological changes in the intervertebral disc. *The Journal of Bone and Joint Surgery* 27,460-73.

Crock, A.O., 1986. Internal disc disruption. A challenge to disc prolapse fifty years on. *Spine* 11, 650-653

De Orio, J.K., Bianco, A.J., 1982. Lumbar disc excision in children and adolescents. *The Journal of Bone and Joint Surgery Am.* 64, 991–996.

Drake, J.D., Aultman, C.D., McGill, S.M., Callaghan, J.P., 2005. The influence of static axial torque in combined loading on intervertebral joint failure mechanics using a porcine model. *Clinical Biomechanics* 20, 1038-1045.

Ebersold, M.J., Quast, L.M., Bianco, A.J., 1987. Results of lumbar discectomy in the pediatric patient. *Journal of Neurosurgery* 67, 643–647.

Galante, J.O., 1967. Tensile properties of the human lumbar annulus fibrosus. *Acta Orthopaedica Scandinavica Suppl.* 100, 5–91.

Ghosh, P. 1988. The Biology of the Intervertebral Disc. CRC Press. Inc. Boca Raton, Florida.

Gordon, S.J., Yang, K.H., Mayer, P.J., et al., 1991. Mechanism of disc rupture- a preliminary report. *Spine* 16 , 450–456.

Guerin, H.A., Elliot, D.M. 2006. Degeneration affects the fiber reorientation of human annulus fibrosus under tensile load. *Journal of biomechanics* 39, 1410-1418.

Gunning, J.L., Callaghan, J.P., McGill, S.M. 2001. Spinal posture and prior loading history modulate compressive strength and type of failure in the spine: a biomechanical study using a porcine cervical spine model. *Clinical Biomechanics* 16, 471-480.

Gunzburg, R., Parkinson, R., Moore, M., Cantraine, F., Hutton,W., Vernon-Roberts, B., Fraser, R., 1992. A cadaveric study comparing discography, magnetic resonance imaging, histology, and mechanical behavior of the human disc. *Spine* 17, 417-426.

Hadler, N. M. 1986. Work disability and musculoskeletal disease. *Arthritis and Rheumatism* 29, 1410-1411.

Hascall,V.C., Lowther, D.A. Biological Mineralization and Demineralization. New York, Springer, 1982, p. 181.)

Haughton,V.M. 1988. MR imaging of the spine. *Radiology* 166, 297-301.

Hasegawa, T., An, H.S., Inufusa, A., Mikawa, Y., Watanabe, R., 2000. The effect of age on inflammatory responses and nerve root injuries after lumbar disc herniation. An experimental study in a canine model. *Spine* 25, 937–940.

Hickey, D,S., Hukins, D.W., 1980. X-ray diffraction studies of the arrangement of collagenous fibres in human fetal intervertebral disc. *Journal of Anatomy* 131, 81-90.

Hickey, D,S., Hukins, D.W., 1980. Relation between the structure of the annulus fibrosus and the function and failure of the intervertebral disc. *Spine* 5, 106-116.

Holm, S., Holm, A.K., Ekström, L., Karlandani, A., Hansson, T., 2004. Experimental disc degeneration due to endplate injury. *Journal of Spinal Disorder*s Technology 17, 64-71.

Hukins, D.W.L. 1988. Disc structure and function. CRC Press, Inc. Boca Raton.

Hsu, E.W, Setton , L.A. 1999. Diffusion tensor microscopy of the intervertebral disc annulus fibrosus. *Magnetic Resonance in Medicine* 41, 992-999.

Iatridis, J.C., Mente, P.L., Stokes, I.A, et al., 1999 .Compression-induced changes in intervertebral disc properties in a rat tail model. *Spine* 24, 996–1002.

Johnson, E.F., Berryman, H., Mitchell, R., Wood, W.W. 1985. Elastic fibres in the annulus fibrosus of the adult human lumbar intervertebral disc. A preliminary report. *Journal of Anatomy* 143, 57-63.

Kirkaldy-Willis W.H. 1988. Managing Low Back Pain, Churchill Livingstone, New York.

Kroeber, M.W., Unglaub, F. , Wang, H., Carsten, C. et al., 2002. New In Vivo Animal Model to Create Intervertebral Disc Degeneration and to Investigate the Effects of Therapeutic Strategies to Stimulate Disc Regeneration. *Spine* 27, 2684–2690.

Lambrigts, D., Sachs, D., Cooper, D., 1998. Discordant organ xenotransplantation in primates. *Transplantation* 66, 547-561.

Lee, J.Y., Ernestus, R.I., Schröder, R., Klug, N. 2000. Histological study of lumbar intervertebral disc herniation in adolescents. *Acta Neurochirurgica (Wien)* 142, 1107-1110.

Lipson, S.J., 1987. Metaplastic proliferative fibrocartilage as an alternative concept to herniated intervertebral disc. *Spine* 13,1055-1060.

Lundin, O., Ekström, L., Hellström, M., Holm,S. Swärd,L., 2000. Exposure of the porcine spine to mechanical compression: differences in injury pattern between adolescents and adults. *European Spine Journal* 9, 466–471.

Marchand, F., Ahmed, A., 1990. Investigation of the laminate structure of lumbar disc annulus fibrosus. *Spine* 15, 402-410.

Marras, W.S., Lavender, S.A., Leurgans, S.E., Rajulu, S.L., Allread, W.G., Fathallah, F.A., Ferguson, S.A. 1993. The role of dynamic three-dimensional trunk motion in occupationally-related low back disorders. The effects of workplace factors, trunk position, and trunk motion characteristics on risk of injury. *Spine* 18, 617-628.

McGill, S.M., 2002. Low back disorders. Evidence-based prevention and rehabilitation. Human Kinetics. Windsor.

Moore, R.J., Vernon-Roberts, B., Fraser, R.D., Osti, O.L., Schembri, M., 1996. The origin and fate of herniated lumbar intervertebral disc tissue. *Spine* 21, 2149-2155.

Murphy, P.L., Volinn, E. 1999. Is occupational low back pain on the rise? *Spine* 24, 691-697.

Norman, R., Wells, R., Neumann, P., Frank, J., Shannon, H., Kerr, M. 1998. A comparison of peak vs cumulative physical work exposure risk factors for the reporting of low back pain in the automotive industry. *Clinical Biomechanics* 13, 561-573.

Neuville, C. 1991.The adult spine; Principles and practice. J.W Frymoyer editor. Raven Press, Ltd, New York.

Osti, O.L., Vernon-Roberts, B., Fraser, R.D., 1990. Anulus tears and intervertebral disc degeneration: An experimental study using an animal model. *Spine* 15, 762-767.

Oxland, T.R., Panjabi, M.M., Southern, E.P., et al., 1991. An anatomic basis for spinal instability: a porcine trauma model. *Journal of Orthopaedic Research* 9, 452–462.

Panjabi, M.M. 1992. The stabilizing system of the spine. Part II. Neutral zone and instability hypothesis. *Journal of Spinal Disorders* 5, 390-397.

Parisini, P., Di Silvestre, M., Greggi,T., Miglietta, A., Paderni, S., 2001. Lumbar disc excision in children and adolescents. *Spine* 26 , 1997-2000.

Parkinson, R.J., Durkin, J.L., Callaghan, J.P., 2005. Estimating the compressive strength of the porcine cervical spine: an examination of the utility of DXA. *Spine* 30, 492-498.

Porter, R.W. 1987. Does hard work prevent disc protrusion? *Clinical Biomechanics* 2, 196-198.

Postacchini, F. 2001. Lumbar disc herniation. A new equilibrium is needed between nonoperative and operative treatment. *Spine* 26, 601.

Punnett, L., Fine, L.J., Keyserling, W.M., Herrin, G.D., Chaffin, D.B., 1991. Back disorders and nonneutral trunk postures of automobile assembly workers. *Scandinavian Journal of Work, Environment and Health.* 17, 337–346.

Reid, J.E,. Meakin, J.R., Robins, S.P,. Skakle, J.M.S., Hukins, D.W.L., 2002. Sheep lumbar intervertebral discs as models for human discs. *Clinical Biomechanics* 17 312–314.

Ross, M., Reith, E., Romrell, L., 1989. Histology; A text and atlas, Williams & Wilkins, Baltimore.

Samstein, B.. Platt, J., 2001. Physiologic and immunologic hurdles to xenotransplantation. *Journal of the American Society of Nephrology* 12, 182-193.

Tsuji, H., Hirano, N., Ohshima, H., Ishihara, H., Terahata, N., Motoe, T,. 1993. Structural variation of the anterior and posterior anulus fibrosus in the development of human lumbar intervertebral disc. *Spine* 18, 204-210.

Willburger, R.E., Ehiosun, U.K., Kuhnen, C., Krämer, J., Schmid, G. 2004. Clinical symptoms in lumbar disc herniation and their correlation to the histological composition of the extruded disc material. Spine 29, 1655-1661.

Yasuma, T., Makino, E., Saito,S., Inui, M., 1986. Histological development of intervertebral disc herniation. *The Journal of Bone and Joint Surgery* 68-A 1066-1072.

Yingling, V.R., Callaghan, J.P., McGill, S.M., 1999. The porcine cervical spine as a reasonable model of the human lumbar spine: an anatomical, geometric, and functional comparison. *Journal of Spinal Disorders* 12, 415–423.